

# Behavior of Coupling Beams Under Load Reversals

by G. B. Barney, K. N. Shiu, B. G. Rabbat,  
A. E. Fiorato, H. G. Russell, and W. G. Corley

PORTLAND CEMENT  ASSOCIATION

*Research and Development / Construction Technology Laboratories*

# Behavior of Coupling Beams Under Load Reversals

by G. B. Barney, K. N. Shiu, B. G. Rabbat,  
A. E. Fiorato, H. G. Russell, and W. G. Corley\*

## HIGHLIGHTS

Eight model reinforced concrete coupling beam specimens were subjected to reversing loads representing those that would occur in beams of coupled structural walls during a severe earthquake. Effects of selected variables on hysteretic response were determined. Controlled variables included shear span-to-effective-depth ratio of the beams, reinforcement details, and size of the confined concrete core. Load versus deflection, strength, energy dissipation, and ductility characteristics were the basic parameters used to evaluate performance.

Beams had a shear span-to-effective-depth ratio of either 1.4 or 2.8, corresponding to span-to-total-depth ratios of 2.5 or 5.0, respectively. Tests indicated that hysteretic performance of beams with conventional reinforcement is limited by deterioration that results in sliding in the hinging region. Full-length diagonal reinforcement significantly improved the performance of short beams. The improvement for long-span beams was less significant. Larger concrete core size improved load retention capacity.

## INTRODUCTION

The Portland Cement Association is conducting a program to develop design criteria for reinforced concrete structural walls used as lateral bracing in earthquake-resistant buildings. The program consists of analytical and experimental investigations of isolated walls, coupled walls, and frame-wall systems. Of primary concern are the strength, energy dissipation capacity, and ductility of walls and wall systems.

As part of the experimental program, tests were conducted to evaluate the behavior of reinforced concrete coupling beams under inelastic load reversals. These tests were made to develop information for use in the investigation of coupled walls.

Coupling beams are used to join adjacent structural walls. Therefore, understanding hysteretic response of coupling beams is a prerequisite to understanding coupled wall response. This report describes the results of tests on eight reinforced concrete coupling beam specimens subjected to static reversing loads.

## Previous Investigations

Investigations by other researchers provided the background information for the test series.

Brown and Jirsa<sup>(1)\*\*</sup> tested doubly reinforced cantilever beams. These tests indicated that under inelastic load reversals, intersecting cracks formed vertical slip planes through the beams. Formation of these planes led to an eventual breakdown in shear transfer as loading progressed. The breakdown intensified as residual tensile strains developed in the longitudinal reinforcement. Decreasing stirrup spacing improved hysteretic response, but did not eliminate sliding shear as the limiting condition. The beams tested had a shear span-to-effective-depth ratio of either 6.0 or 3.0. Maximum nominal shear stresses ranged from  $2\sqrt{f'_c}$  psi to  $7\sqrt{f'_c}$  psi (0.17  $\sqrt{f'_c}$  MPa to 0.58  $\sqrt{f'_c}$  MPa).

Tests by Paulay and Binney<sup>(2)</sup> on deep coupling beams with conventional reinforcement also resulted in sliding shear failures. To prevent sliding shear, Paulay and Binney used full-length diagonal reinforcement. This arrange-

ment altered the load transfer mechanism to that of a Mesnager hinge. For similar load histories, diagonally reinforced beams sustained their load capacity over a greater number of load cycles and dissipated more energy than conventionally reinforced beams. The beams each had a shear span-to-effective-depth ratio of approximately 0.9. Maximum nominal shear stresses ranged from  $9\sqrt{f'_c}$  psi to  $14\sqrt{f'_c}$  psi (0.75  $\sqrt{f'_c}$  MPa to 1.16  $\sqrt{f'_c}$  MPa).

Bertero and Popov<sup>(3)</sup> investigated other arrangements of special reinforcement using cantilever beams with a shear span-to-effective-depth ratio of 3.1. Maximum loads on the beams were equivalent to nominal shear stresses of approximately  $6\sqrt{f'_c}$  psi (0.5  $\sqrt{f'_c}$  MPa).

In addition to closely spaced confinement hoops with supplementary cross-ties, Bertero and Popov tested beams with supplementary diagonal reinforcement within the hinging region. Their results showed that the ability of the beams to maintain load and dissipate energy was significantly improved by reducing tie spacing. They also determined that diagonal web reinforcement in combination with vertical ties minimized stiffness loss and stabilized hysteretic response under increasing inelastic loading cycles.

Wight and Sozen<sup>(4)</sup> tested a series of columns under large deflection reversals. The specimens were tested as cantilevers with and without axial compressive forces. The shear span-to-effective-depth ratio for the tests was 3.5. Maximum nominal shear ranged from  $4\sqrt{f'_c}$  to  $6\sqrt{f'_c}$  psi (0.33  $\sqrt{f'_c}$  to 0.5  $\sqrt{f'_c}$  MPa). These tests verified that a progressive decrease in strength and stiffness occurs with cycling in the inelastic range. The hysteretic response improved when transverse reinforcement was used to confine the concrete core and carry the total shear. However, providing trans-

\*Respectively, Manager, Building Design Section; Structural Engineer and Senior Structural Engineer, Structural Development Department; Manager, Construction Methods Section; Director, Structural Development Department; and Divisional Director, Engineering Development Division, Portland Cement Association, Skokie, Illinois.

\*\*Superscript numbers in parentheses designate references at the end of this bulletin.

**TABLE 1. Test Program Variables**

Specimen	Core width <i>a</i> (in.)	Span length <i>b</i> (in.)	Primary reinforcement
C1	2.63	16.67	
C2	2.63	16.67	
C3	2.63	16.67	
C4	3.50	16.67	
C5	3.50	16.67	
C6	3.50	16.67	
C7	3.50	33.33	
C8	3.50	33.33	

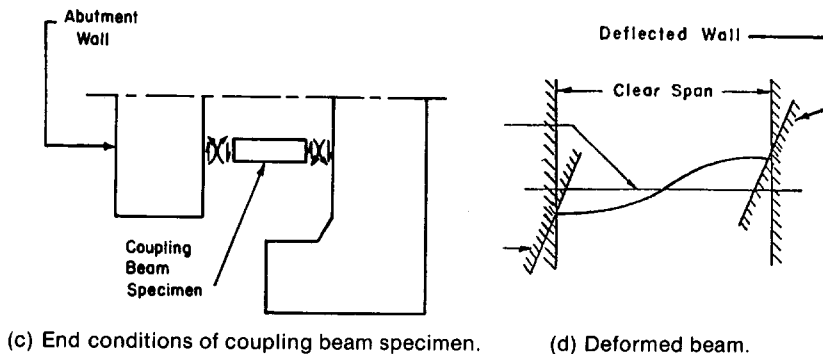
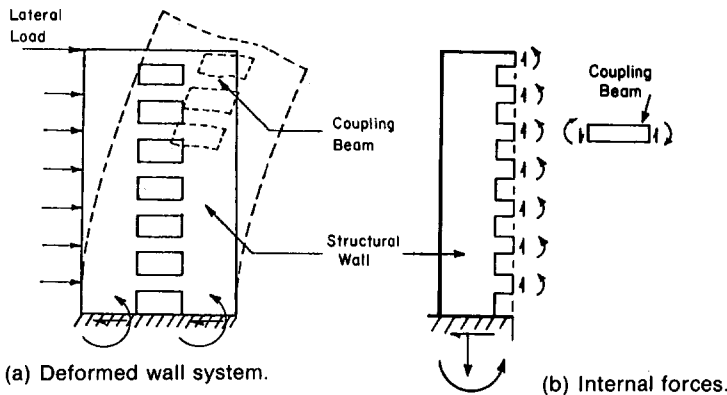
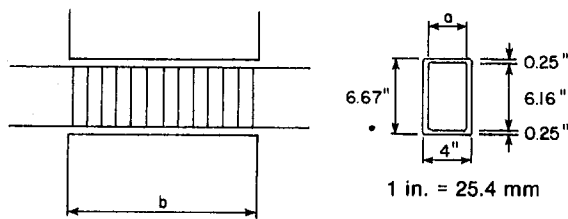


**Fig. 1. Idealized coupling beam deformations and forces.**

verse reinforcement to carry the entire shear did not eliminate the possibility of shear failure with large load reversals. Because the concrete core must remain intact to carry the shear, effective confinement of the core is essential.

Although the tests described in this report are an extension of previous investigations, they were planned as part of an overall program on earthquake resistance of structural walls. Therefore, the design of the specimens incorporated details for a future test program on coupled-wall systems.

**Objectives and Scope**

The objectives of this investigation were

1. To provide information for selecting details of coupling beams for use in tests of structural wall systems.
2. To determine strengths of coupling beams subjected to reversing loads.
3. To determine load-versus-deflection characteristics of coupling beams with various reinforcing details.
4. To determine ductility and energy-dissipation capacities of coupling beams subjected to reversing loads.

Eight specimens were tested. They represented approximately one-third-scale models although no specific prototypes were considered. Specimens were subjected to in-plane reversing loads simulating those in beams of coupled structural walls.

Controlled variables in the program were the type and arrangement of primary reinforcement, span-to-depth ratio, and size of confined concrete core. Details of specimens are listed in Table 1.

This report includes a description of the experimental program and the observed response of the test specimens. Effects of controlled variables are analyzed. Strength, load-versus-deflection relationships, energy dissipation, and ductility were the basic parameters used to evaluate performance.

**OUTLINE OF EXPERIMENTAL PROGRAM**

This section gives a brief description of the test specimens and test procedure. A more detailed description can be found in Appendix A.

## Test Specimens

The configuration of the test specimens was selected so that applied loads and deformations represented those on beams in coupled walls subjected to lateral forces. Beam deformations and forces were idealized as shown in Fig. 1. The test specimen is shown in Fig. 2. Each specimen consisted of two coupling beams framing into abutment walls at each end. End conditions imposed by the abutments represented those at the beam-wall intersection of coupled walls. Axial forces in coupling beams were not considered in this investigation.

The beams had rectangular cross sections 4 in. (102 mm) wide and 6.67 in. (169 mm) deep. The effective depth of the main longitudinal reinforcement was 6.1 in. (155 mm). Beam lengths were 16.67 in. (423 mm) or 33.33 in. (847 mm). These corresponded to shear span-to-effective-depth ratios of 1.4 and 2.8, respectively. The L-shaped abutment walls were 4 in. (102 mm) thick. Overall specimen dimensions are given in Fig. 3.

## Specimen Design

The short coupling beams were designed to carry maximum forces corresponding to nominal shear stresses of approximately  $9\sqrt{f'_c}$  psi ( $0.75\sqrt{f'_c}$  MPa). For design purposes, concrete strength was taken as 3000 psi (20.7 MPa) and steel yield strength as 60 ksi (414 MPa). Steel strain hardening of 50% was assumed. Primary reinforcement was selected to develop capacities corresponding to the desired maximum shear stress levels. To avoid anchorage failures, development lengths were 50% greater than those required by the 1971 ACI Building Code.<sup>(5)</sup>

Transverse-hoop reinforcement was provided in all specimens to resist shear and to confine the concrete core. The hoops consisted of D-3 deformed wire spaced 1.33 in. (34 mm) on centers. Design of the reinforcement was such that stresses in the hoops were below yield at forces corresponding to the maximum capacity of the beams. Shear stresses were calculated using Equation 11-3 of the 1971 ACI Building Code with the capacity reduction factor,  $\Phi$ , equal to 1.0. Shear reinforcement was proportioned according to Equation 11-13 of the 1971 ACI Building Code. Nominal

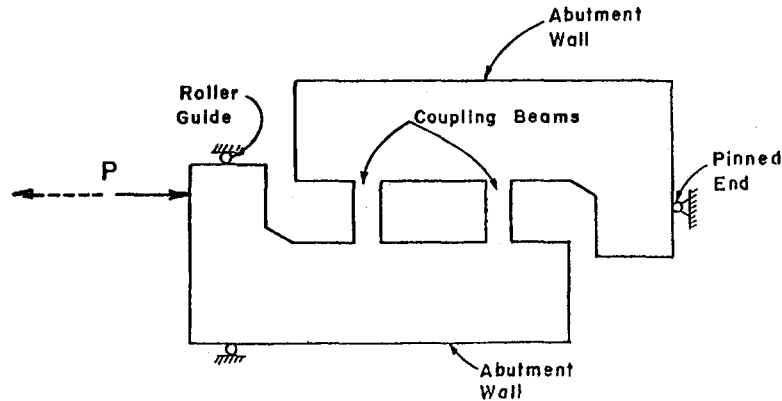


Fig. 2. Test specimen.

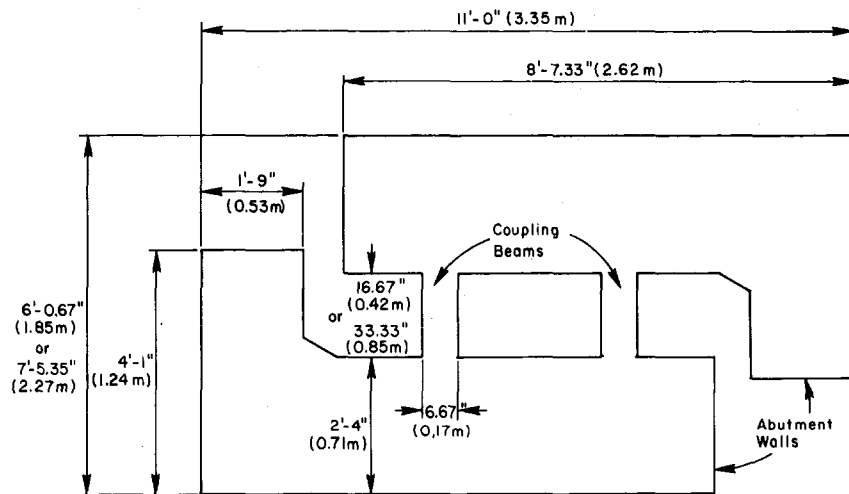


Fig. 3. Specimen geometry.

concrete shear stress capacity was neglected. The hoops also met the requirements for transverse reinforcement in flexural members of special ductile frames in Section A.5 of the 1971 ACI Building Code.

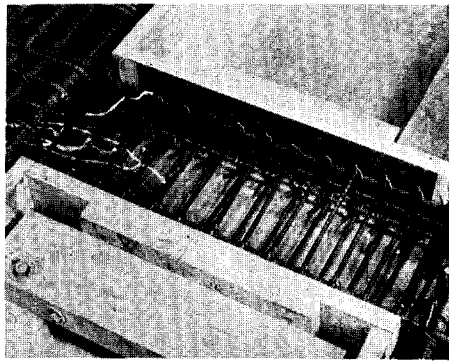
**Specimens C2, C5, and C7.** Specimens C2, C5, and C7 had straight longitudinal reinforcement, consisting of four 6-mm-diameter ( $\frac{1}{4}$ -in.) bars top and bottom. Photographs of the reinforcement are shown in Fig. 4(a) and (b). A larger confined concrete core was provided for Specimens C5 and C7. Shear span-to-effective-depth ratio of Specimens C2 and C5 was 1.4. For Specimen C7, the ratio was 2.8.

**Specimens C1, C3, and C4.** Specimens C1, C3, and C4 had diagonal bars in the hinging regions. This reinforcement was provided to reduce shear deterioration

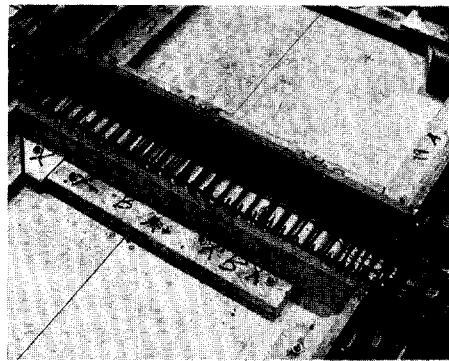
as suggested in tests by Bertero and Popov.<sup>(3)</sup> Design of these bars was based on the assumption that they would behave as diagonal truss members after the concrete deteriorated under repeated load reversals. They were designed to carry the maximum shear force without yielding. For Specimen C1, two 6-mm-diameter ( $\frac{1}{4}$ -in.) bars from both top and bottom were bent at  $45^\circ$  starting at the face of the wall at each end of the beam as shown in Fig. 4(c). Specimens C3 and C4 contained two additional 6-mm ( $\frac{1}{4}$ -in.) bars top and bottom bent at  $45^\circ$ . A photograph of this reinforcement for Specimen C4 is shown in Fig. 4(d). Additional reinforcement details are presented in the Appendix.

**Specimens C6 and C8.** Specimens C6 and C8 had full-length diagonal reinforcement. This detail was used by

#### 4 Behavior of Coupling Beams Under Load Reversals



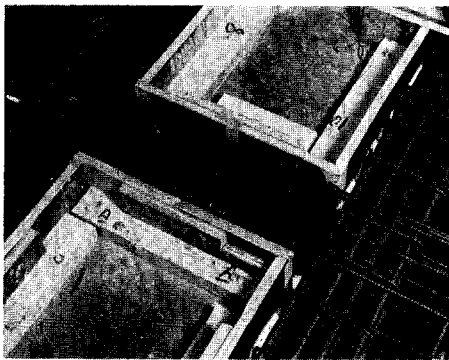
(a) Specimen C2



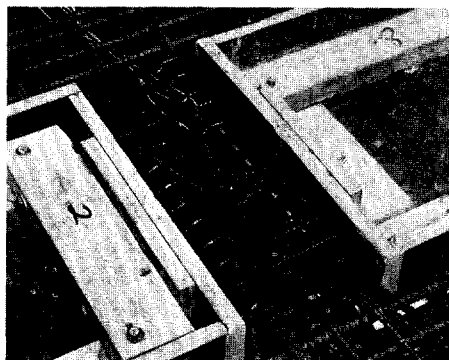
(b) Specimen C7



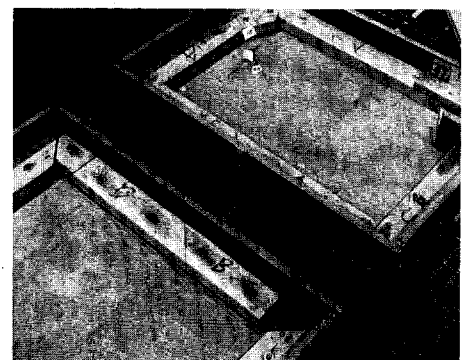
(c) Specimen C1



(d) Specimen C4



(e) Specimen C6



(f) Specimen C8

Fig. 4. Reinforcement for test specimens.

Paulay and Binney<sup>(2)</sup> for coupling beams with shear span-to-effective-depth ratios less than 0.9. Specimens C6 and C8 had shear span-to-effective-depth ratios of 1.4 and 2.8, respectively.

Full-length diagonals for short beam specimens were designed to carry the maximum shear force corresponding to a nominal stress of  $9\sqrt{f'_c}$  psi ( $0.76\sqrt{f'_c}$  MPa). The area of diagonal reinforcement,  $A_s$ , was calculated as

$$A_s = \frac{V_u}{2f_s \sin \alpha} \quad (1)$$

where  $V_u$  = maximum shear force  
 $f_s$  = stress in diagonal reinforcement (90 ksi; 621 MPa)  
 $\alpha$  = angle between diagonal bar and horizontal

Using this approach, a single No. 4 bar was provided in one direction and two No. 3 bars were used in the opposite direction.

Transverse hoops were provided to contain concrete in the core during reversals and to prevent buckling of the diagonal bars. Longitudinal bars supporting transverse hoops were not anchored in the abutment walls.

The reinforcement details used for Specimens C6 and C8 are shown in Fig. 4(e) and (f).

#### Test Procedure

The test setup is shown in Fig. 5. Specimens were placed parallel to the laboratory floor and supported on thrust bearings. Loads were applied by hydraulic rams at one end and resisted by a fixed support at the opposite end. The line of action of forces passed through the mid-length of the coupling beams.

Loading was controlled by the magnitude of applied force prior to yielding and by imposed deflections after yielding. For each increment of applied load or deflection, three completely reversed

load cycles were applied. This is illustrated in Fig. 6. Deflections in successive increments were increased until the specimen was destroyed.

Instrumentation was provided to measure applied loads, deflections, beam elongations, and reinforcing steel strains.

#### GENERAL RESPONSE CHARACTERISTICS

In evaluating the test results, applied load was assumed to divide equally between the two beams in each specimen. This assumption was checked by comparing companion measurements from each beam and by visual observation of the beams during testing. Except for Specimen C3, the performance of the two beams in each specimen was similar. In Specimen C3, one of the beams deteriorated more rapidly than the other after the maximum load was

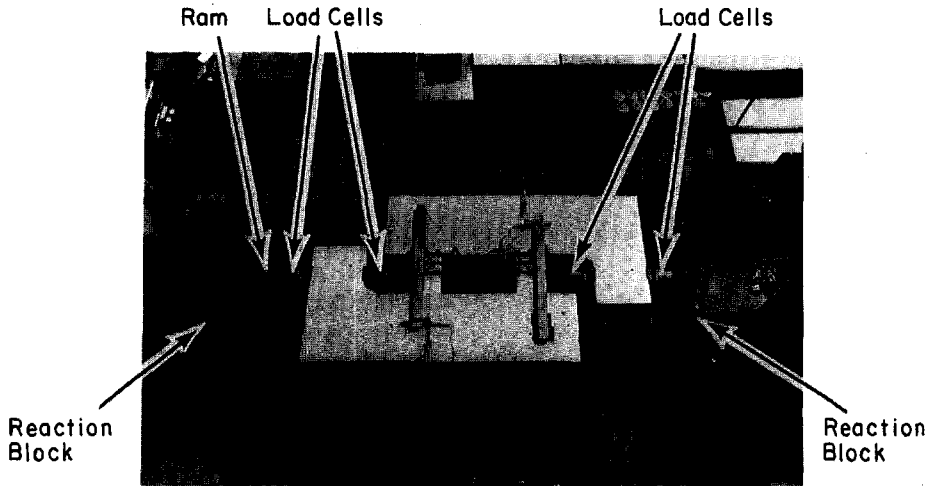


Fig. 5. Test setup.

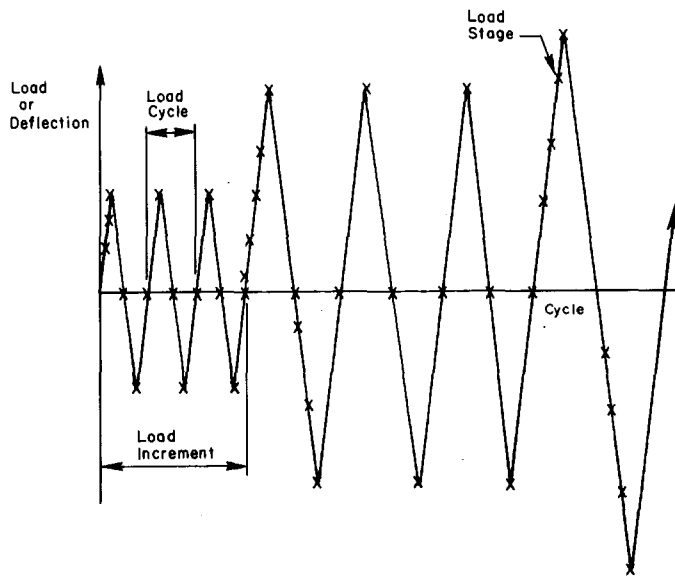


Fig. 6. Load or deflection history.

reached. Test results for this specimen must be considered accordingly.

**Conventional Longitudinal Reinforcement**

Specimens C2, C5, and C7 had conventional longitudinal reinforcement. Specimens C2 and C5 had short-span beams and core widths of 2.63 and 3.50 in. (67 and 89 mm), respectively. Specimen C7 had long-span beams and a core width of 3.50 in. (89 mm). Load-versus-deflection relationships for the specimens are

shown in Figs. 7, 8, and 9. Plotted loads are those for each beam. Deflections are the relative displacements between ends of the beams.

Performance of the beams with conventional straight longitudinal reinforcement was limited by deterioration of the shear-resisting mechanism in the hinging region. Under reversing loads, intersecting cracks developed across the entire depth of the beams at their ends. As subsequent inelastic load reversals were applied, concrete at the ends was

destroyed by cracking, abrasion, and spalling. With the concrete destroyed, shear transfer by truss action was not possible and the transverse hoops became ineffective. Interface shear transfer also was lost. Eventually, dowel action of longitudinal reinforcement provided the primary shear resistance. This loss of shear transfer is often termed sliding-shear behavior. Because sliding developed along a plane parallel to the transverse reinforcement, even the closely spaced hoops became inefficient in transmitting shear. However, the hoops did provide confinement of the concrete core.

Deterioration of the concrete at the ends of the beams was intensified by elongation of the beams, caused by residual tensile strains in the longitudinal reinforcement. These strains developed with successive load reversals into the inelastic range. In addition, partial slip of reinforcement anchored in the abutment walls contributed to widening cracks at the ends of the beams. Slip developed as bond between concrete and reinforcement deteriorated under inelastic load reversals.

Degradation of the shear-transfer mechanism and deterioration of the confined concrete core were associated with "pinching" of the load-versus-deflection loops shown in Figs. 7, 8, and 9. The pinching occurred because, as loads were reversed, slip along the interface took place with little increase in load. Eventually, concrete surfaces on either side of the interface were brought into contact with each other and the load resistance increased. In addition, shear transfer by dowel action of the longitudinal reinforcement increased. As the number of load cycles increased, continued abrasion and crushing of concrete in the critical region resulted in a complete breakdown of the shear-transfer mechanism at the interface.

Both short- and long-span coupling beams exhibited pinching. However, it was somewhat less severe for the long-span beams.

**Diagonal Reinforcement in Hinging Regions**

To improve the performance of short-span beams, diagonal reinforcement was provided in the hinging region of several specimens. This reinforcement

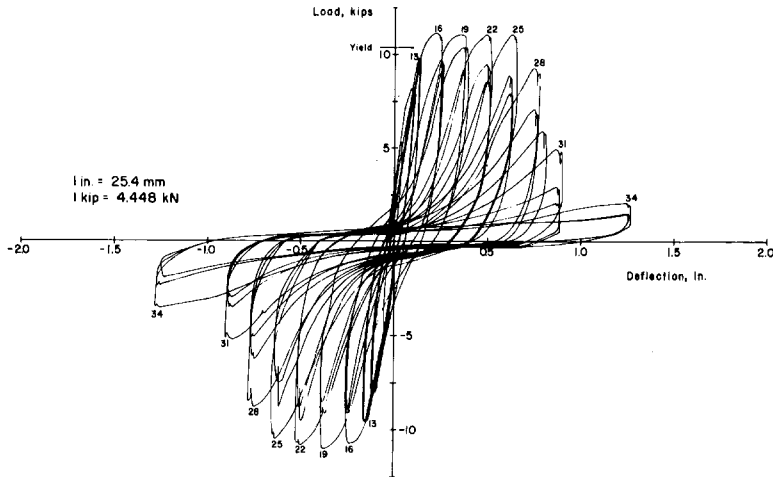


Fig. 7. Load-versus-deflection relationship for Specimen C2.

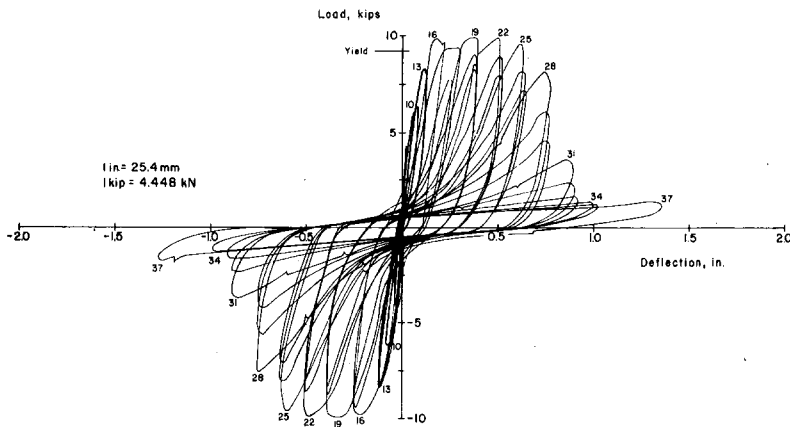


Fig. 8. Load-versus-deflection relationship for Specimen C5.

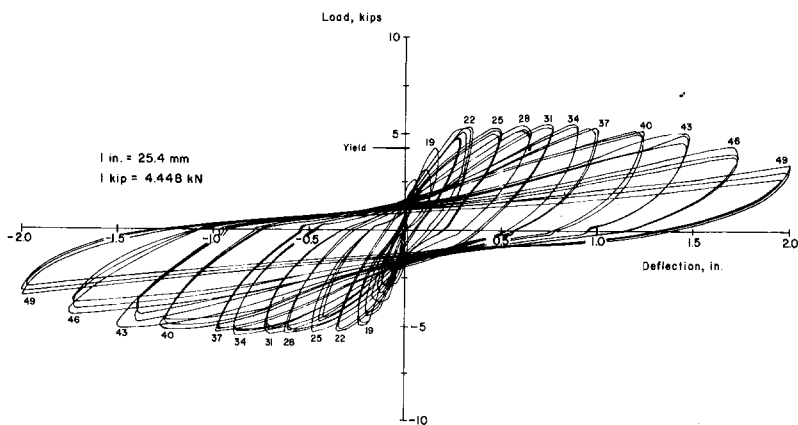


Fig. 9. Load-versus-deflection relationship for Specimen C7.

was patterned after details tested by Bertero and Popov.<sup>(3)</sup> However, modifications were made to simplify fabrication.

Specimens C1, C3, and C4 had diagonal reinforcement in the hinging regions as indicated in Fig. 4 and Table 1. Specimens C1 and C3, with the smaller core size, had single and double diagonal bars, respectively. Specimen C4, with the larger core size, had double diagonal bars.

The diagonal reinforcement was intended to eliminate the sliding shear that limited inelastic response of the beams with conventional horizontal reinforcement. Diagonal reinforcement was designed to provide an internal truss system to resist shear and to move the critical plastic hinge location away from the face of the wall.

Use of diagonal reinforcement in the hinging regions did not result in the anticipated improvement in performance. The unsatisfactory performance was caused by factors discussed below.

The hysteretic response of Specimens C1, C3, and C4 is illustrated in the load-versus-deflection relationships shown in Figs. 10, 11, and 12, respectively. Comparison of these figures with those shown previously for short-span beams with conventional reinforcement indicates that the special diagonals did not significantly improve the hysteretic response characteristics. The few improvements in energy dissipation and load retention capacities that were attained do not seem to warrant the added complexity and cost of the diagonals.

The primary reason that the diagonals within the hinging region did not perform satisfactorily lies in the details for tying the truss together. Initially, the beams behaved as expected. Tensile yielding of the flexural reinforcement at the face of the wall and at the intersection of the diagonals occurred almost simultaneously. As loading cycles progressed into the inelastic range, concrete within the region of the diagonals deteriorated by spalling and crushing.

In principle, loss of concrete should not have affected the ability of the diagonal trusses to resist load as long as the diagonal bars did not buckle. However, as loading progressed and concrete was lost, the support points for the diagonals loosened, allowing the corners of the diagonal bars to become displaced.

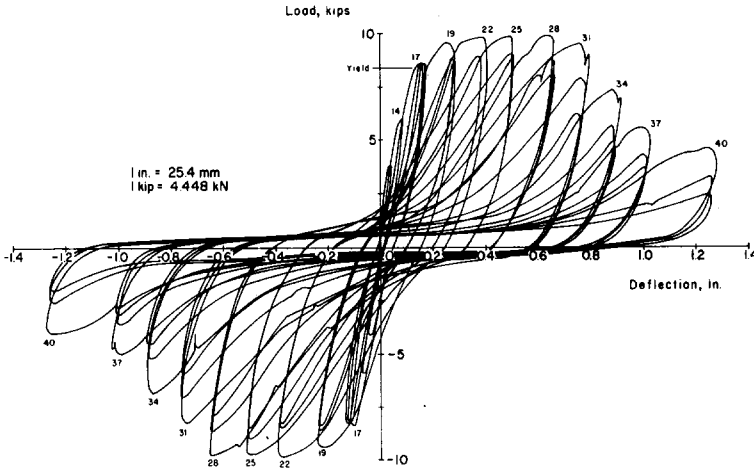


Fig. 10. Load-versus-deflection relationship for Specimen C1.

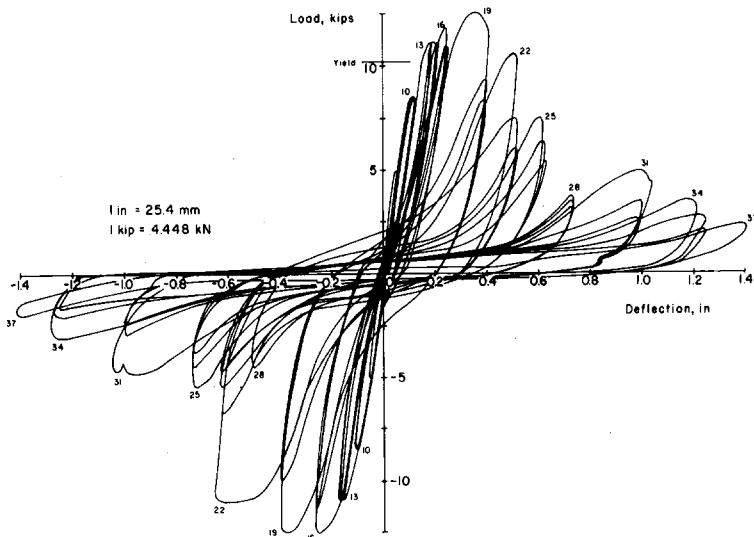


Fig. 11. Load-versus-deflection relationship for Specimen C3.

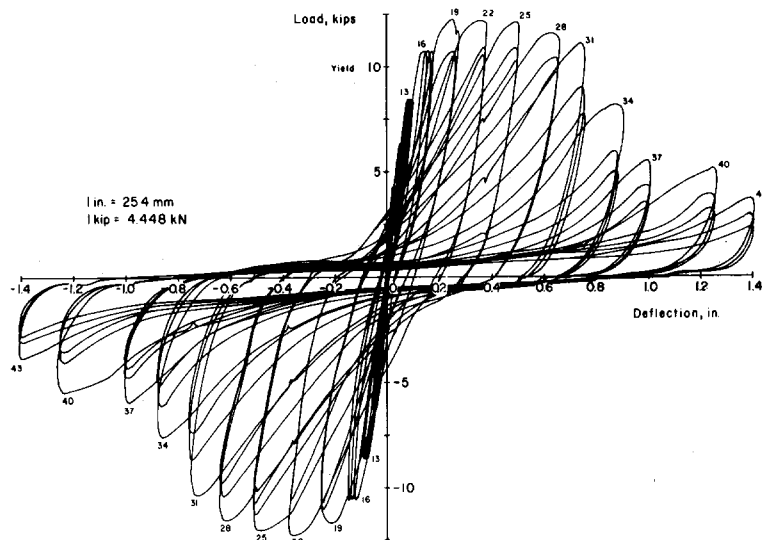


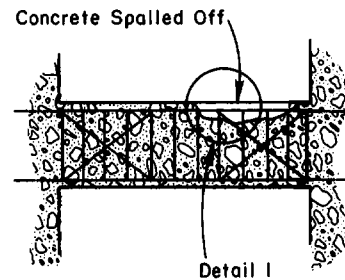
Fig. 12. Load-versus-deflection relationship for Specimen C4.

(See Fig. 13.) Once the supports for the diagonal truss softened, efficient truss action could not be developed. Therefore, the diagonals were not effective in carrying the applied shear.

It should be noted that the transverse hoops located at the corners of the diagonal were adequate for resisting the outward thrust of the diagonal bars. Strain measurements indicated that these hoops did not yield. The problem encountered was that the force in the diagonal was not effectively transmitted to the transverse hoop.

The addition of a second set of diagonals in Specimens C3 and C4 was attempted in order to lower the force levels in the diagonal bars. However, the result was not satisfactory. It is apparent that in using this type of diagonal reinforcement, extreme caution must be exercised in securing the bars. The effectiveness and cost-to-benefit ratio of this detail are questionable.

One method of improving this detail would be to eliminate the bend in the diagonals at the intersection of the beam with the wall. However, this would cause additional problems in fabrication of beam and wall reinforcement.



(a) General Location

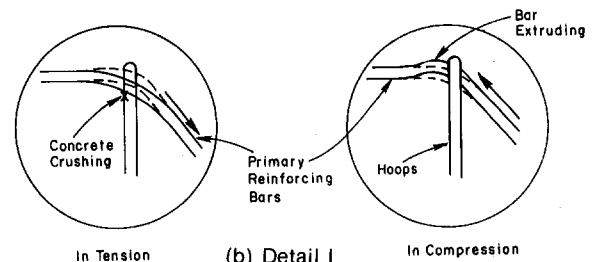


Fig. 13. Loss of support for diagonals in hinging region.

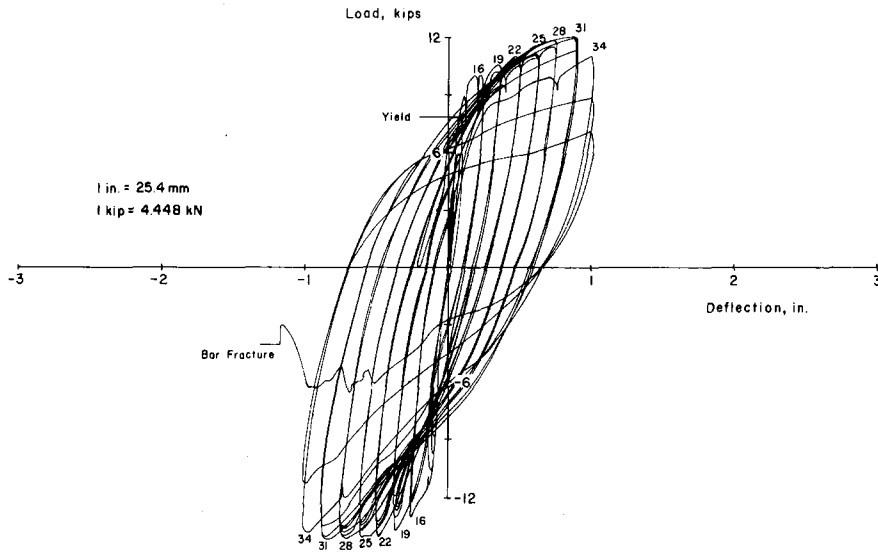


Fig. 14. Load-versus-deflection relationship for Specimen C6.

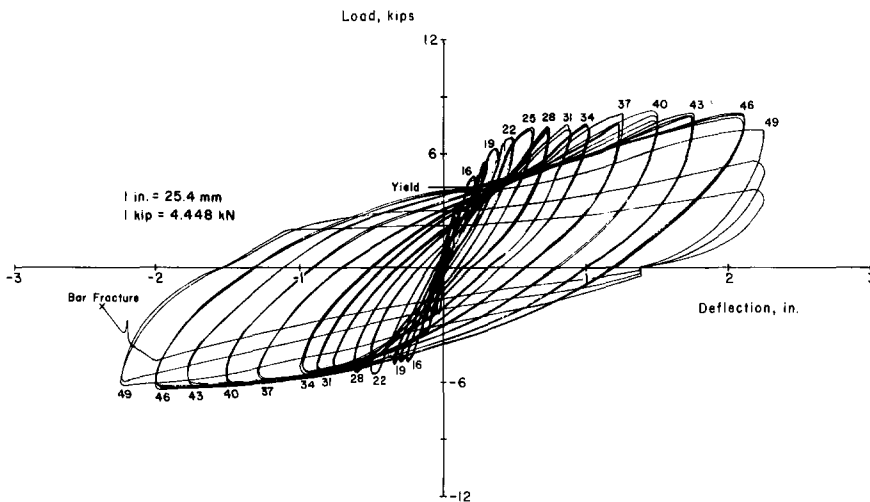


Fig. 15. Load-versus-deflection relationship for Specimen C8.

### Full-Length Diagonal Reinforcement

Because of the ineffectiveness of diagonals located in the hinging regions and the sliding shear limitation with conventional reinforcement, Specimens C6 and C8 were tested with full-length diagonal reinforcement. The beams had shear span-to-effective-depth ratios of 1.4 and 2.8, respectively. Reinforcement details are given in Fig. 4 and Table 1. The straight longitudinal bars supporting the transverse hoops were not anchored in the abutment walls and were

not considered to contribute to the load-resisting mechanism.

Load-versus-deflection relationships for Specimens C6 and C8 are shown in Figs. 14 and 15. Full-length diagonals effectively increased the load-retention and energy-dissipation capacities of these coupling beams. The load-versus-deflection curves do not exhibit the pinching that results from deterioration of the shear-resisting mechanism. Also, the sliding-shear mechanism leading to loss of stiffness and strength was not observed.

Initial cracking in the beams with full-

length diagonals was similar to that observed in the beams with conventional reinforcement. As inelastic load cycles were applied, concrete at the beam-wall interface crushed and spalled. This deterioration, however, was not reflected in the load-versus-deflection relationships. Forces on the beams were effectively resisted by truss action of the diagonal bars. The transverse hoops contained the concrete core over most of the beam, thus preventing the diagonal bars from buckling.

Performance of test beams with full-length diagonals was eventually limited by inelastic buckling and subsequent fracture of the diagonal bars. At later stages of the test, concrete spalling at the beam-wall intersection exposed the diagonal bars within the abutment wall. In this region no reinforcement was provided to prevent the diagonals from buckling.

The mechanism that develops with use of full-length diagonals is essentially that of a Mesnager hinge. It was expected, based on Paulay and Binney's tests,<sup>(2)</sup> that significant improvement in response would be observed in the short-span beams. The shear span-to-effective-depth ratio of these beams was 1.4 as compared to a maximum ratio of 0.9 in the beams studied by Paulay and Binney.<sup>(2)</sup> The use of full-length diagonals in longer-span beams had not been tested previously. Therefore, Specimen C8 was tested with a shear span-to-effective-depth ratio of 2.8.

Based on the behavior of Specimens C7 and C8, the improvement obtained using full-length diagonals in beams with a shear span-to-effective-depth ratio of 2.8 (span-to-depth ratio of 5.0) was relatively small. In addition, gravity loads within the span take on greater significance for longer-span beams. These loads cannot be resisted efficiently by diagonal reinforcement. Considering these findings, full-length diagonal bars do not appear to be justified for coupling beams with shear span-to-effective-depth ratios of 2.8 or greater.

### STRENGTH CHARACTERISTICS

Table 2 is a summary of yield and maximum loads for the test specimens. Observed and calculated values are given. They represent the load on each beam

TABLE 2. Specimen Strengths

Specimen No.	Yield load					Maximum load					Observed maximum Observed yield
	Observed		Calculated*		Observed Calc.	Observed		Calculated*		Observed Calc.	
	kips	$\sqrt{f'_c}$	kips	$\sqrt{f'_c}$		kips	$\sqrt{f'_c}$	kips	$\sqrt{f'_c}$		
C1	8.1	6.2	9.0	6.9	0.90	9.2	7.0	10.8	8.2	0.85	1.13
C2	10.2	7.6	9.8	7.3	1.04	10.3	7.7	12.8	9.6	0.80	1.01
C3	10.2	7.7	9.8	7.4	1.04	11.8	9.0	12.4	9.4	0.95	1.17
C4	10.0	7.0	9.5	6.7	1.05	11.5	8.0	11.7	8.2	0.98	1.14
C5	9.2	6.7	8.8	6.5	1.05	9.4	6.8	11.4	8.4	0.82	1.01
C6	7.8	6.3	7.4	6.0	1.05	13.4	10.9	14.4	11.6	0.93	1.73
C7	4.3	2.9	4.4	3.0	0.98	5.2	3.5	5.6	3.8	0.93	1.21
C8	4.3	3.0	4.0	2.8	1.08	7.5	5.3	8.7	6.1	0.86	1.77

1 kip = 4.448 kN;  $1\sqrt{f'_c}$  (psi) =  $0.0830\sqrt{f'_c}$  (MPa)

\*Based on monotonic flexural response.

based on the assumption that the total load was distributed equally. The area used to calculate the nominal shear stress was the width of the beam times its effective depth.

### Observed Strengths

Yield loads given in Table 2 are those observed when the main flexural reinforcement first reached its yield strain. For most specimens, the main flexural reinforcement was the straight longitudinal bars. For Specimens C6 and C8, which had full-length diagonals, yield load is that observed when the diagonal bars reached their yield strain.

Maximum observed loads correspond to the maximum value measured in either direction of loading. The last column in Table 2 gives the ratio of observed maximum load to the observed yield load for each specimen.

Several observations can be made regarding the strengths of the test specimens. For the short-span beams with conventional longitudinal reinforcement, Specimens C2 and C5, maximum load was only 1% higher than the yield load. This is indicative of the sliding-shear deterioration that occurred in the cycles subsequent to yield.

Beams in Specimen C7, which had long spans with conventional reinforcement, reached a maximum load 21% greater than yield load.

Specimens C1, C3, and C4, which had short-span beams with diagonal reinforcement in the hinging regions, reached maximum loads 13% to 17%

greater than yield loads.

Specimens C6 and C8, with full-length diagonals, had ultimate strengths 73% to 77% greater than their yield strengths. This indicates that the diagonal bars developed strain hardening efficiently. In designing coupled-wall systems, differences between ultimate strength and yield strength must be recognized because forces developed in the beams influence the performance of the walls.

As indicated earlier, the hoop reinforcement was designed so that it would not yield at loads corresponding to the capacity of the beams. Strain measurements<sup>(6)</sup> confirmed that the hoops did not yield for either conventionally reinforced beams or those with special reinforcement. It is apparent that transverse hoops cannot prevent sliding shear in short, conventionally reinforced beams when repeated inelastic load reversals are applied. However, this is dependent on load history. The laboratory loading on the beams was intentionally severe.

### Calculated Strengths

Calculated values of yield load and maximum load, shown in Table 2, were based on measured material properties. The calculated values are estimates of monotonic flexural strength. They do not account for effects of load reversals. Loads for Specimens C6 and C8, with full-length diagonals, were estimated using Equation (1).

Calculated flexural yield values are in basic agreement with observed values.

Observed maximum loads range from 80% to 98% of calculated loads. Besides the normal variations expected in such calculations, the differences reflect the effects of load reversals and shear deterioration.

Nominal shear stresses, given in Table 2, were based on the effective depth of the section and the overall beam width. Observations of the beams during testing indicated that the concrete shell surrounding the confined core broke away during the inelastic load cycles. At this stage, nominal shear stresses based on the area of the confined core are more realistic. For Specimens C1, C2, and C3, the core area was 66% of the nominal area. Thus, nominal shear stresses based on the area of the confined core are 1.5 times those in Table 2. Based on the core area, maximum nominal stresses observed in C1, C2, and C3 were  $10.7\sqrt{f'_c}$  psi,  $11.7\sqrt{f'_c}$  psi, and  $13.7\sqrt{f'_c}$  psi ( $0.89\sqrt{f'_c}$  MPa,  $0.97\sqrt{f'_c}$  MPa, and  $1.14\sqrt{f'_c}$  MPa), respectively.

For all other specimens, the core area was 88% of the nominal area. The corresponding maximum nominal shear stress for short-span beams ranged from  $7.8\sqrt{f'_c}$  to  $12.5\sqrt{f'_c}$  psi ( $0.65\sqrt{f'_c}$  to  $1.04\sqrt{f'_c}$  MPa). For long-span beams, the range was from  $4.0\sqrt{f'_c}$  to  $6.1\sqrt{f'_c}$  psi ( $0.33\sqrt{f'_c}$  to  $0.52\sqrt{f'_c}$  MPa).

### DEFORMATION CHARACTERISTICS

Because of potential excursions into the inelastic range of response, deformation

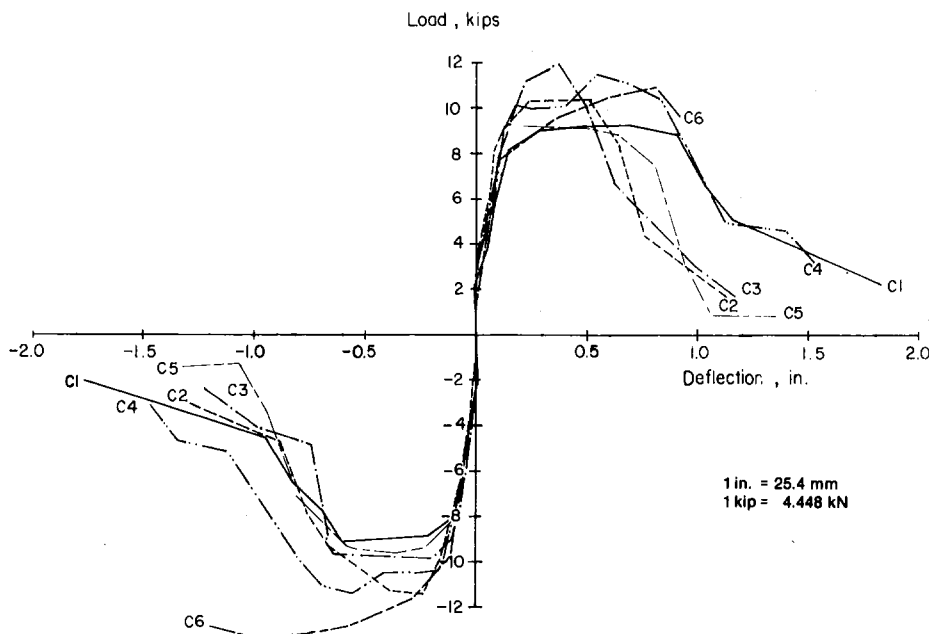


Fig. 16. Load-versus-deflection envelopes for specimens with short-span beams.

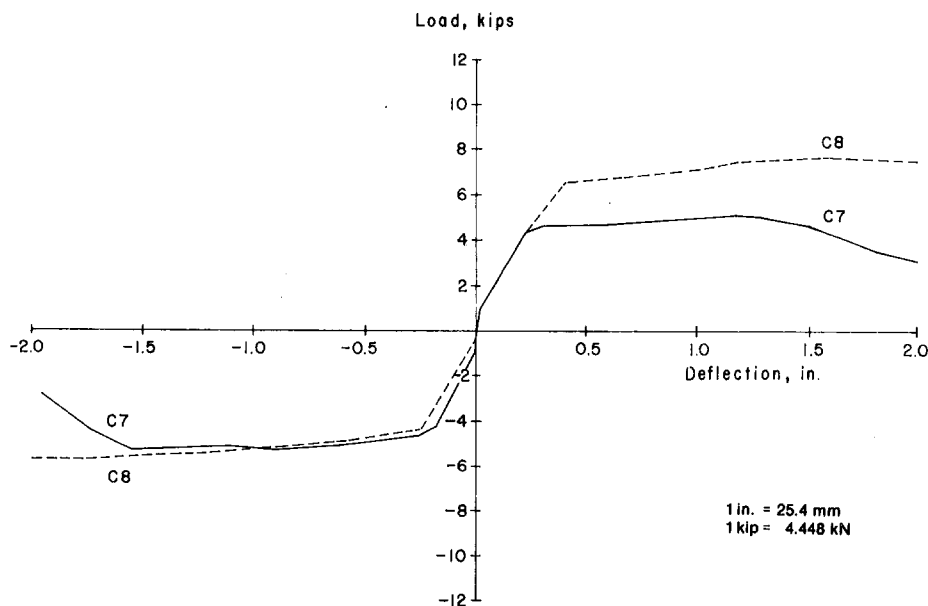


Fig. 17. Load-versus-deflection envelopes for specimens with long-span beams.

characteristics of coupling beams are of considerable interest. For the beams tested, these characteristics have been quantified in terms of overall-load-versus-deflection relationships, energy dissipation, and ductility.

**Load-Versus-Deflection Envelopes**

Figs. 16 and 17 show envelopes of the load-versus-deflection relationships for the short-span and long-span beams, respectively.

Except for Specimen C6, beams with shear span-to-effective-depth ratios of 1.4 reached their maximum load capacities at deflections between 0.4 and 0.5 in. (10 and 13 mm). These deflections corresponded to overall rotations of 0.02 and 0.03 radian. Overall rotations were calculated as deflection divided by length of beam.

Specimen C7, which had conventional longitudinal reinforcement and a shear span-to-effective-depth ratio of 2.8, reached its maximum load at a deflection of 0.9 in. (23 mm). This corresponded to an overall rotation of 0.03 radian.

Specimens C6 and C8, with full-length diagonals, reached maximum load capacities at deflections of 0.8 in. (20 mm) and 1.5 in. (38 mm), respectively. Corresponding rotations were 0.05 radian for both the short-span and long-span specimens. Although beams with full-length diagonals reached higher rotations at maximum load than did other beams, their final load loss was more sudden. This is because their load capacity was limited by bar fracture.

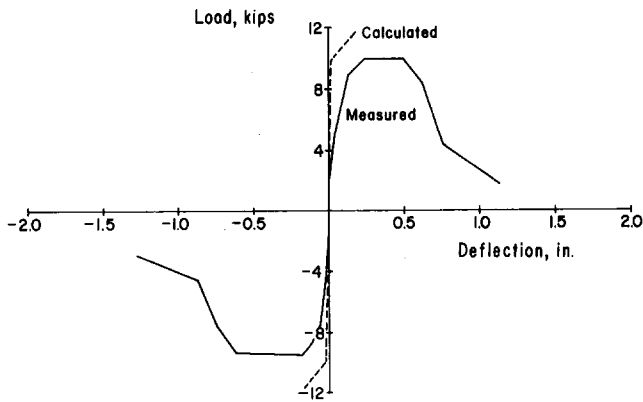
It is evident in Figs. 16 and 17 that the envelopes for Specimens C6 and C8 are not symmetrical for opposite directions of loading. This is because the areas of the diagonal reinforcement were not equal. Two No. 3 bars were used in one diagonal direction and one No. 4 bar was used in the other direction. The areas for these bars were 0.22 and 0.20 sq in. (142 and 129 mm<sup>2</sup>), respectively.

Measured load-versus-deflection envelopes are compared with calculated envelopes in Figs. 18 and 19. The calculated curves represent first-order approximations for monotonically loaded beams. Only flexural deformations were considered.<sup>(6)</sup> Calculated curves are presented to illustrate that the beam deformations are made up of a number of components, not all of which are quantifiable.

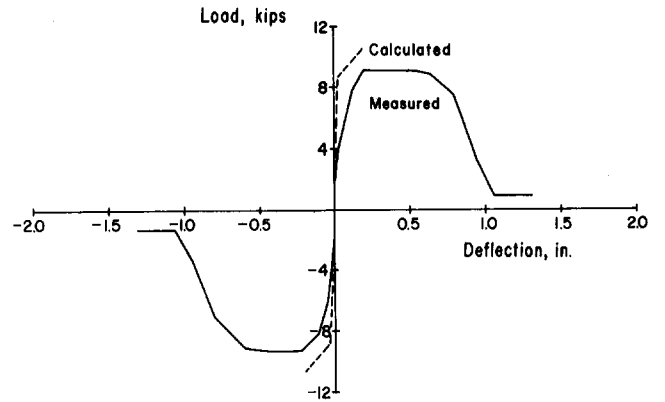
Measured deflections are considerably in excess of calculated values, particularly for the short-span beams. The following factors, not included in the calculations, could make a significant contribution to the deflection.

1. Shearing distortions
2. Slip of main reinforcement anchored in abutment walls
3. Load reversals

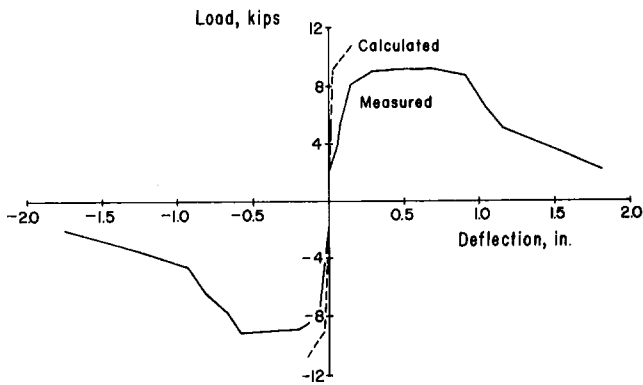
In addition, there are normal limita-



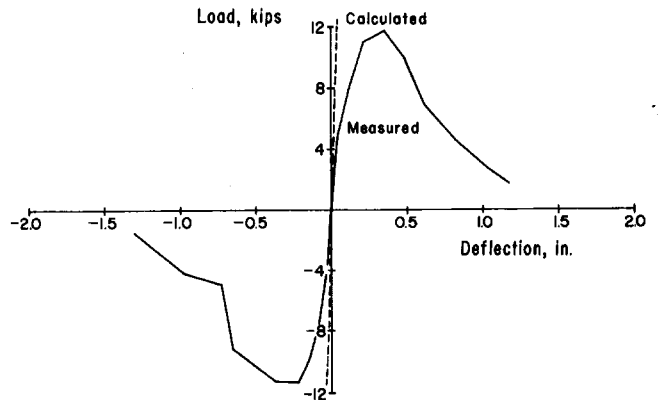
(a) Specimen C2



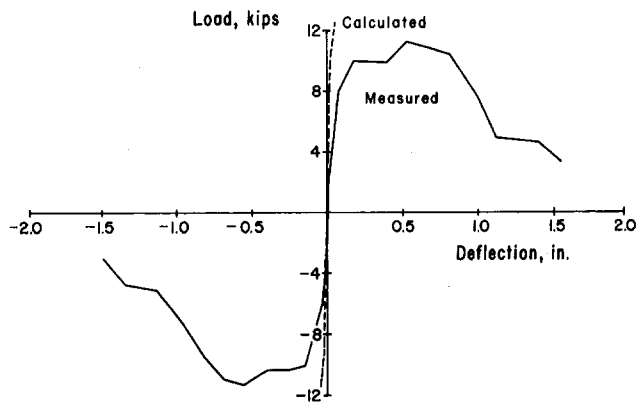
(b) Specimen C5



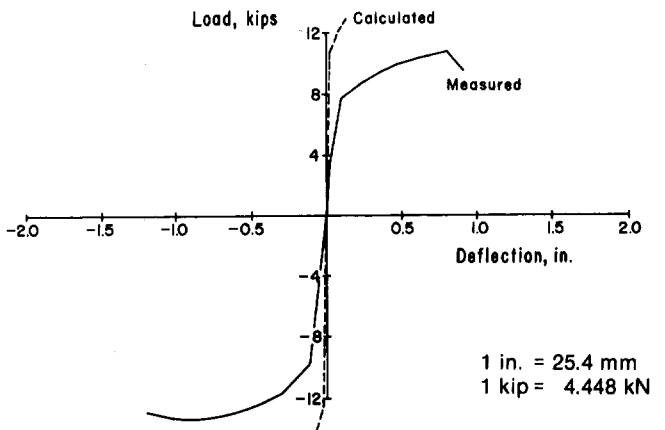
(c) Specimen C1



(d) Specimen C3



(e) Specimen C4



(f) Specimen C6

1 in. = 25.4 mm  
1 kip = 4.448 kN

**Fig. 18. Calculated and measured load-versus-deflection envelopes for short-span beams.**

tions on the accuracy of deflection calculations.

The influence of shearing distortions can be seen in Figs. 18 and 19. Calculated deflections for Specimen C7 are in

better agreement with measured values than are those for Specimen C5. It would be expected that shearing distortions would have less influence on Specimen C7 with more slender beams.

For the short beams with conventional reinforcement, the contribution of shearing distortions was estimated using the procedure developed by Bachmann.<sup>(7)</sup> The modified calculations<sup>(6)</sup>

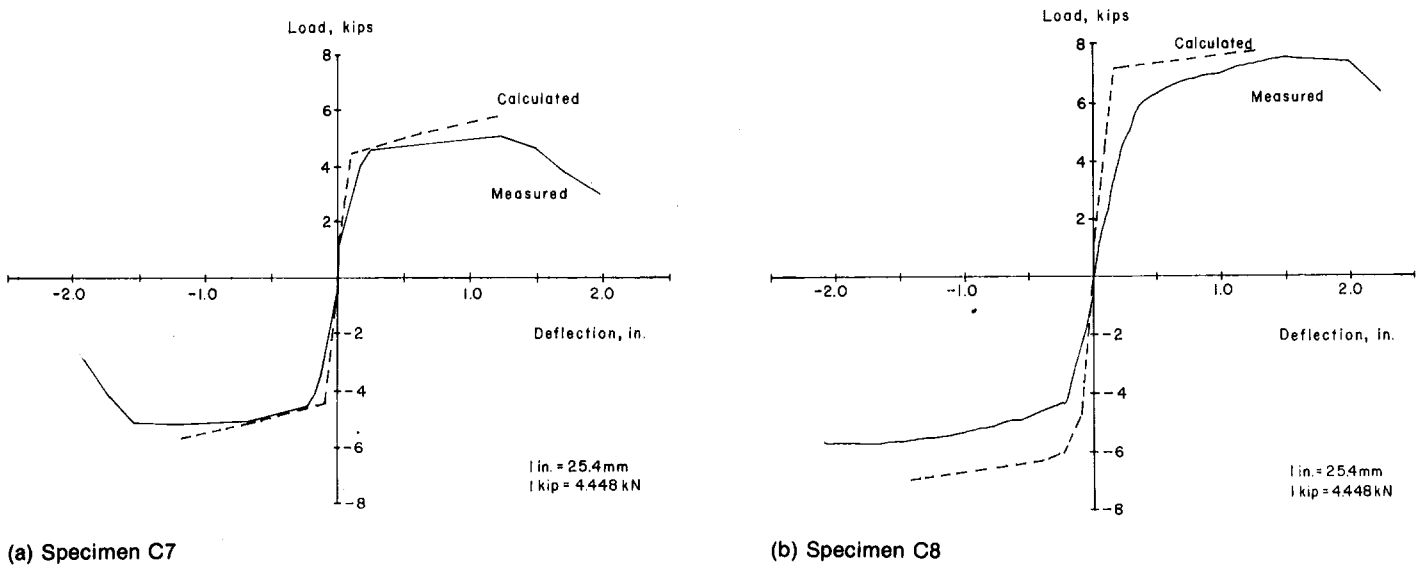


Fig. 19. Calculated and measured load-versus-deflection envelopes for long-span beams.

are a better approximation of the envelope, as shown in Figs. 20 and 21. Again, load reversals were not taken into account.

To be more than just a relative measure of performance, the calculation of load-versus-deflection relationships for beams under load reversals requires extensive refinement. Such refinement is outside the scope of this project.

**Ductility**

The ductility of a structure is commonly used as a measure of its inelastic performance. Deflection ductility ratio is

defined in this report as the ratio of the deflection of the beams to the deflection measured at yield. Cumulative deflection ductility ratio is the summation of ductility ratios for each cycle of loading. (See Fig. 22.) Ductility ratios for positive and negative loadings are added separately.

Comparisons of the performance of specimens based on cumulative ductility are shown in Fig. 23, where the load is plotted as a percentage of the maximum, observed in either loading direction.

Specimens C2 and C5 with short-span beams and conventional reinforcement were tested with confined core area equal to 66% and 88% respectively,

of the effective section area. As shown in Fig. 23(a), the larger confined core area improved behavior. Under load reversals, the concrete shell fell off. Thus, nominal shear stresses on the smaller core were larger and lower cumulative ductility was attained.

The effects of different reinforcement arrangements on ductility are shown in Figs. 23(b) and 23(c) for the short-span and long-span beams, respectively. For the short-span beams, the specimen with full-length diagonals maintained its load capacity for a significantly larger ductility than the other specimens. The difference was not as significant for the long-span beams.

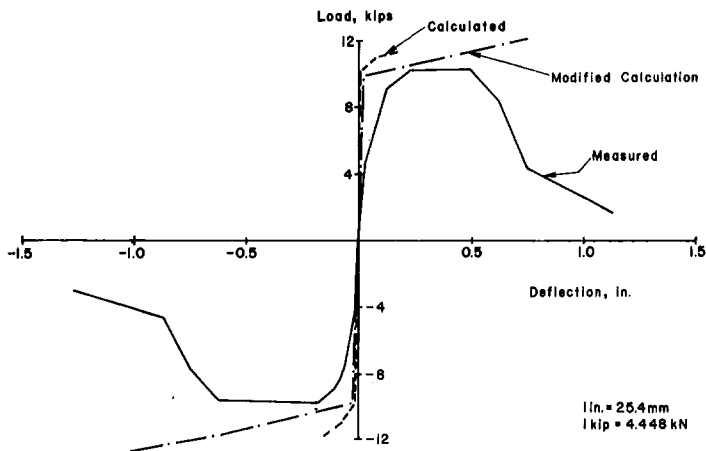


Fig. 20. Influence of diagonal cracking on the calculation of deflection for Specimen C2.

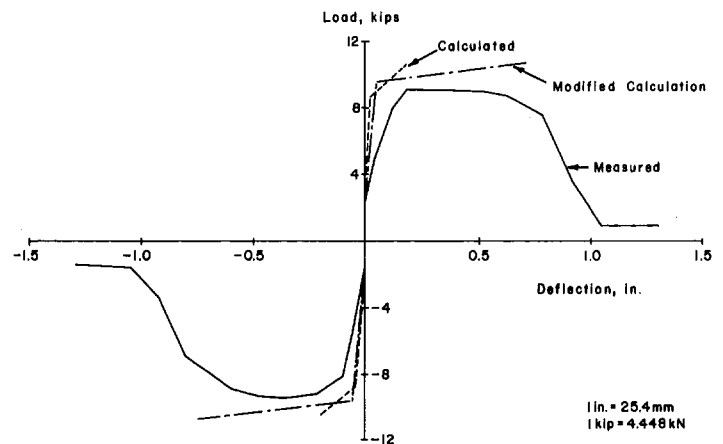


Fig. 21. Influence of diagonal cracking on the calculation of deflection for Specimen C5.

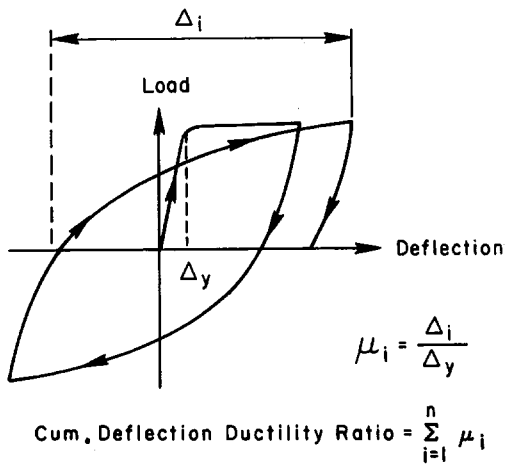


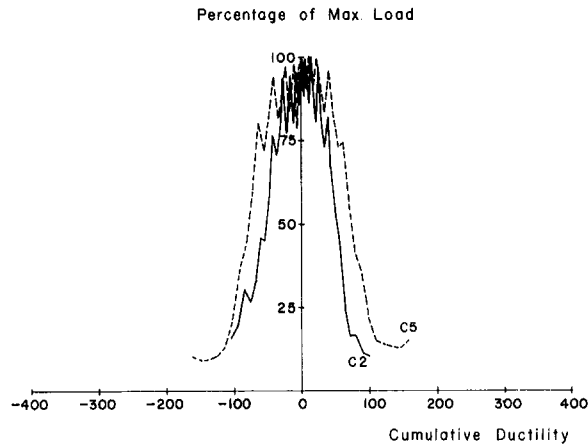
Fig. 22. Cumulative deflection ductility ratio.

**Energy-Dissipation Capacity**

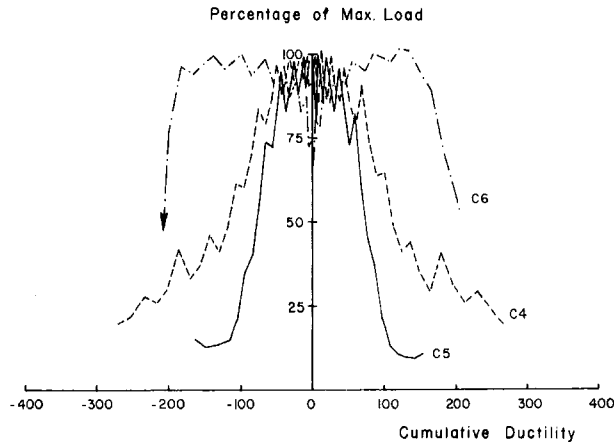
Energy dissipation provides a measure of the inelastic performance of a structure under load reversals. The dissipated energy is the difference between that expended during load application and that recovered during unloading. Energy dissipation is thus defined as the area enclosed by the load-versus-deflection loops. (See Fig. 24.) Using the energy dissipation derived from the measured load-versus-deflection relationships of the test specimens provides a convenient reference for quantifying the specimens' performance. Essentially, for equivalent loads and deflections, specimens dissipating the most energy would be considered to have the best performance.

Figs. 25 and 26 illustrate the "stability" of the load-versus-deflection loops for the specimens. In the loading sequence, three complete cycles of load or deflection were applied at each load deflection increment. Figs. 25 and 26 show the cumulative energy dissipated for the first, second, and third cycles of each increment. Energy dissipation is plotted against displacement ductility ratio. Displacement ductility ratio is defined as the deflection at each increment divided by the yield deflection.

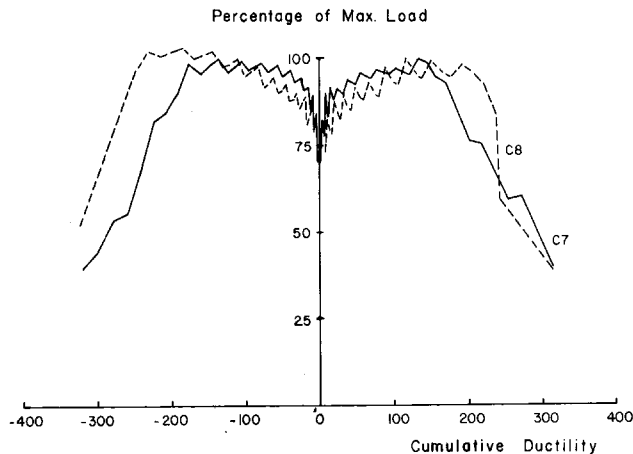
If the three loops within each increment had identical areas for each cycle, it would mean that there was no loss of energy-dissipation capacity. As can be seen in Figs. 25(f) and 26(b), this was nearly the case for Specimens C6 and



(a) Effect of core size for short-span beams.



(b) Effect of reinforcement for short-span beams.



(c) Effect of reinforcement for long-span beams.

Fig. 23. Load versus cumulative deflection ductility.

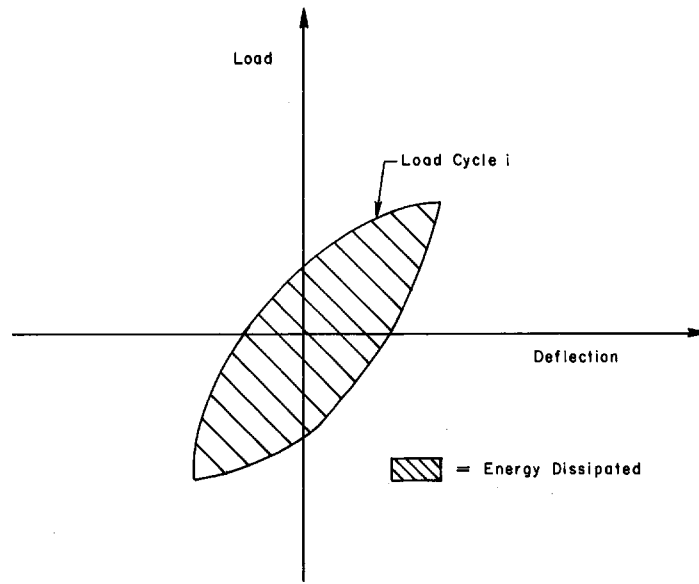
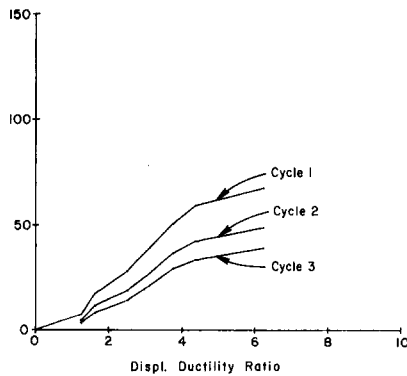


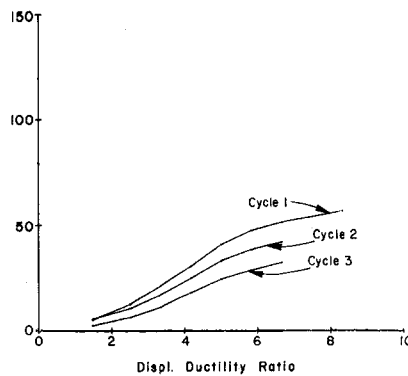
Fig. 24. Energy dissipation.

Cumulative Energy Dissipation, in-kips



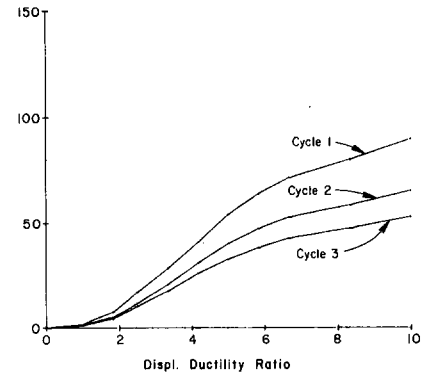
(a) Specimen C2

Cumulative Energy Dissipation, in-kips



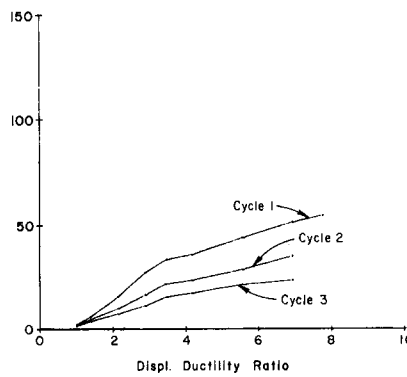
(b) Specimen C5

Cumulative Energy Dissipation, in-kips



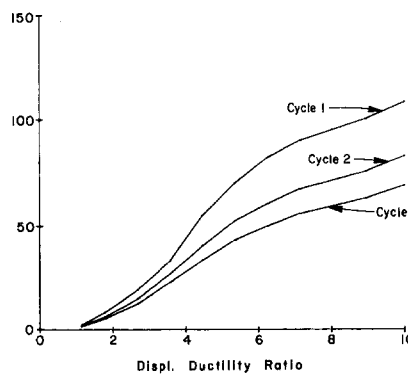
(c) Specimen C1

Cumulative Energy Dissipation, in-kips



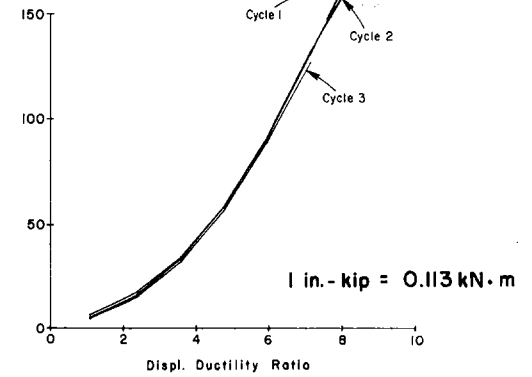
(d) Specimen C3

Cumulative Energy Dissipation, in-kips



(e) Specimen C4

Cumulative Energy Dissipation, in-kips



(f) Specimen C6

Fig.25. Energy dissipation versus displacement ductility ratio for short-span beams.

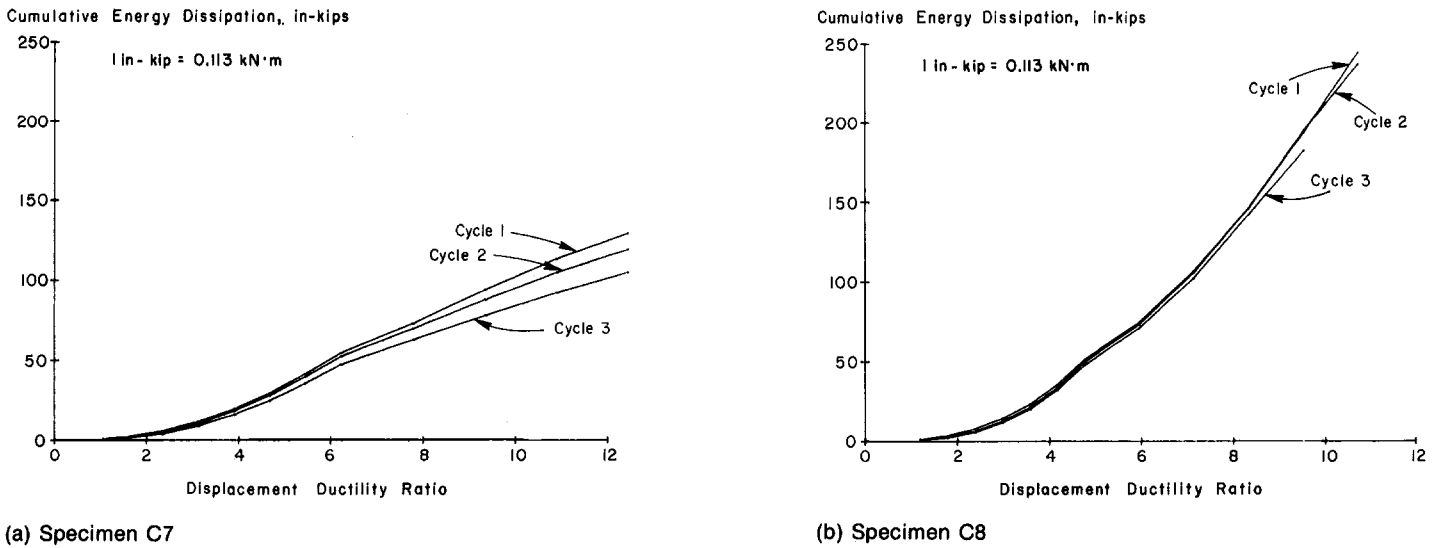


Fig. 26. Energy dissipation versus displacement ductility ratio for long-span beams.

C8, which had full-length diagonals. The wider differentials between successive cycles within each load increment for the other beams attested to the greater deterioration of these beams. The curves in Figs. 25 and 26 illustrate more clearly what was indicated in the load-versus-deflection relationships presented earlier.

While Figs. 25 and 26 show the performance of each specimen, they do not give the relationships between the various specimens. These relationships can be shown by normalizing the cumulative energy dissipated by the product of the yield load and yield deflection, as follows:

$$E_{mn} = \frac{1}{P_y \Delta_y} \sum_{i=1}^n e_i \quad (2)$$

- where  $E_{mn}$  = normalized cumulative energy dissipated
- $P_y$  = yield load
- $\Delta_y$  = yield deflection
- $e_i$  = energy dissipated in  $i$ th load cycle
- $i$  = number of load cycles

Figs. 27 and 28 show the normalized cumulative energy dissipated versus number of cycles for the short-span and long-span beams, respectively. All load cycles are included in the cumulative energy determination. Since the specimens had similar load histories, these curves provide a comparative measure of the energy dissipation capacity of the test specimens.

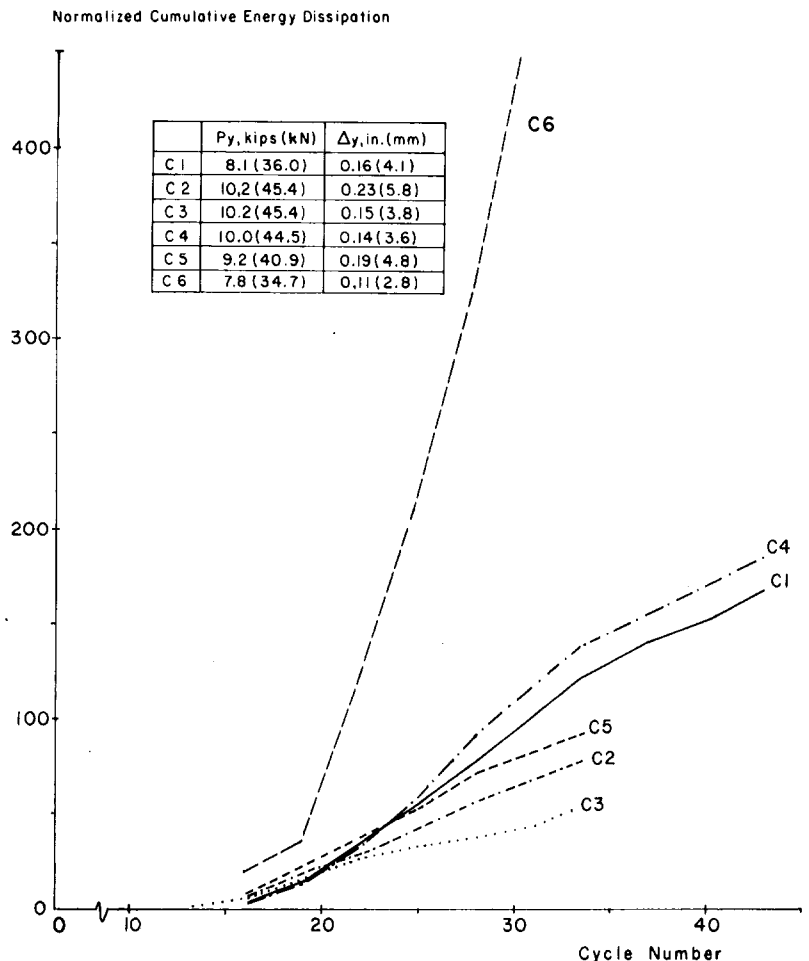


Fig. 27. Normalized cumulative energy dissipation versus cycle number for short-span beams.

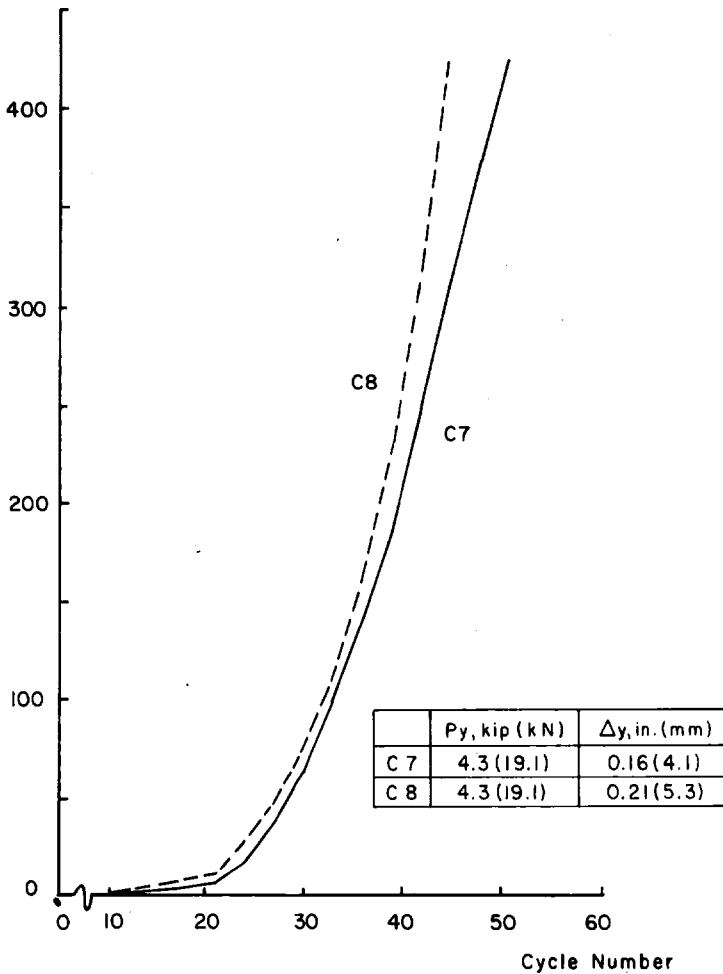


Fig. 28. Normalized cumulative energy dissipation versus ductility for long-span beams.

Energy-dissipation-versus-ductility relationships confirm the results previously indicated. For short-span beams, Specimen C6 with full-length diagonals provided the greatest energy-dissipation capacity. Special diagonals within the hinging regions improved energy-dissipation capacity somewhat, but the improvement was not great enough to justify their complexity and cost.

For the long-span beams, the full-length diagonals did not provide significant additional energy-dissipation capacity.

**SUMMARY AND CONCLUSIONS**

Eight model reinforced concrete coupling-beam specimens were subjected to

reversing loads representing those that would occur in beams of coupled structural walls during a severe earthquake. The beams were constructed at approximately one-third scale. Effects of selected variables on hysteretic response were determined. Controlled variables included shear span-to-effective-depth ratio of the beams, reinforcement details, and size of the confined concrete core. The variables are summarized in Table 1.

The beams had a shear span-to-effective-depth ratio of either 1.4 or 2.8, corresponding to a span-to-depth ratio of 2.5 or 5.0. Maximum nominal shear stress on short-span beams ranged from  $7\sqrt{f'_c}$  psi ( $0.58\sqrt{f'_c}$  MPa) for beams with conventional reinforcement to  $11\sqrt{f'_c}$  psi ( $0.91\sqrt{f'_c}$  MPa) for beams with full-length diagonal reinforcement. Equiva-

lent shear stresses for long-span beams were  $4\sqrt{f'_c}$  psi and  $5\sqrt{f'_c}$  psi ( $0.33\sqrt{f'_c}$  MPa and  $0.42\sqrt{f'_c}$  MPa).

Load-versus-deflection relationship, strength, energy dissipation, and ductility were the basic parameters used to evaluate performance of the test specimens. The following conclusions are based on the test results.

**Conventional Longitudinal Reinforcement**

Inelastic response of coupling beams with conventional reinforcement was limited by sliding-shear deterioration at the beam-wall intersection. This was the case even though transverse hoops were provided to carry the entire shear without yielding. Since sliding-shear cracks developed between transverse reinforcement, the hoops eventually became ineffective. Development of sliding shear is dependent on load history. Deterioration is a function of the cycle number and the intensity of applied loads. Thus, any generalization of the results must consider load history. Both the number of cycles and the load intensity used in the laboratory tests can be considered as representative of extremely severe earthquake conditions on the most critically stressed beam in a coupled-wall system.

Specimen C5, which had short-span beams, sustained an overall rotation of 0.025 radian. At this rotation increment more than 80% of the maximum load was maintained for three complete cycles. Yield rotation for Specimen C5 was 0.01 radian.

Specimen C7, which had long-span beams, sustained an overall rotation of 0.04 radian. Yield rotation for this specimen was 0.005 radian.

Tests indicated that improved inelastic performance was obtained by increasing the size of the concrete core. The confined core of coupling beams should be made as large as possible within the limits of cover requirements.

**Diagonal Reinforcement In Hinging Regions**

Diagonal reinforcement within hinging regions at the ends of the beams improved performance, but not enough to justify the added complexity and cost.

To use this type of reinforcement, extreme care must be exercised in the selection and construction of details, particularly at bend locations in the reinforcement. Based on the laboratory tests, it does not appear that this detail would be an economical solution.

### Full-Length Diagonal Reinforcement

Beams with full-length diagonal reinforcement had the best strength, ductility, and energy-dissipation characteristics of any of those tested.

Specimen C6, which had short-span beams, sustained an overall rotation of 0.05 radian. Yield rotation for this specimen was 0.01 radian.

Specimen C8, which had long-span beams, sustained an overall rotation of 0.06 radian. Yield rotation was 0.01 radian. Improvement in hysteretic response using full-length diagonals for long-span beams was not as significant as for short-span beams. In addition, gravity loads within the span took on greater significance for longer-span beams. These loads cannot be resisted efficiently by diagonal reinforcement. Thus, straight diagonal bars do not appear to be justified for beams with a shear span-to-effective-depth ratio of 2.8 or more. Tests using this type of reinforcement have not been carried out on coupling beams with a shear span-to-effective-depth ratio between 1.4 and 2.8.

If full-length diagonals are used, the diagonal bars must be properly anchored in the adjoining wall. The diagonals must be restrained over their full length to prevent buckling.

Since this type of detail effectively developed strain hardening of the reinforcement, the actual capacity of the beams should be considered in designing a structural wall system. A design based on yield level would not properly allow for the forces that can be imparted to the walls by the beams.

### Final Remarks

The results of these tests have clearly indicated the relative influence of special reinforcement details on inelastic hysteretic response of coupling beams. However, the results do not justify the use of one system over the other for all

situations. The response characteristics and energy-dissipation capacity attainable in the beams must be matched with those required for the structure and the design conditions under consideration.

For example, for very short beams under severe earthquake loads, full-length diagonals may provide the best solution. In other situations, however, conventionally reinforced beams might be adequate. Also, consideration must be given to the fact that not all beams over the height of a coupled-wall system are subjected to the same load histories.

### ACKNOWLEDGMENTS

Investigation reported here was carried out at the Structural Development Department of the Portland Cement Association. Fabrication and testing of the specimens were performed by the technical staff of the department under the direction of laboratory foreman B. W. Fullhart.

The work was part of a combined analytical and experimental investigation sponsored by the National Science Foundation under Grant No. ENV74-14766 and by the Portland Cement Association. Mark Fintel was overall project director. The opinions, findings, and conclusions expressed in this publication are those of the authors and do not necessarily reflect the views of the National Science Foundation.

### REFERENCES

1. Brown, R. H., and Jirsa, J. O., "Reinforced Concrete Beams Under Load Reversals," *Journal of the American Concrete Institute, Proceedings*, Vol. 68, No. 5, May 1971, pages 380-390.
2. Paulay, T., and Binney, J. R., "Diagonally Reinforced Coupling Beams of Shear Walls," *Shear in Reinforced Concrete*, Publication SP-42, American Concrete Institute, Detroit, 1974, pages 579-598.
3. Bertero, V. V., and Popov, E. P., "Hysteretic Behavior of Reinforced Concrete Flexural Members with Special Web Reinforcement," *Proceedings*, U.S. National Conference on Earthquake Engineering, Ann Arbor, Mich., June 1975, pages 316-326.

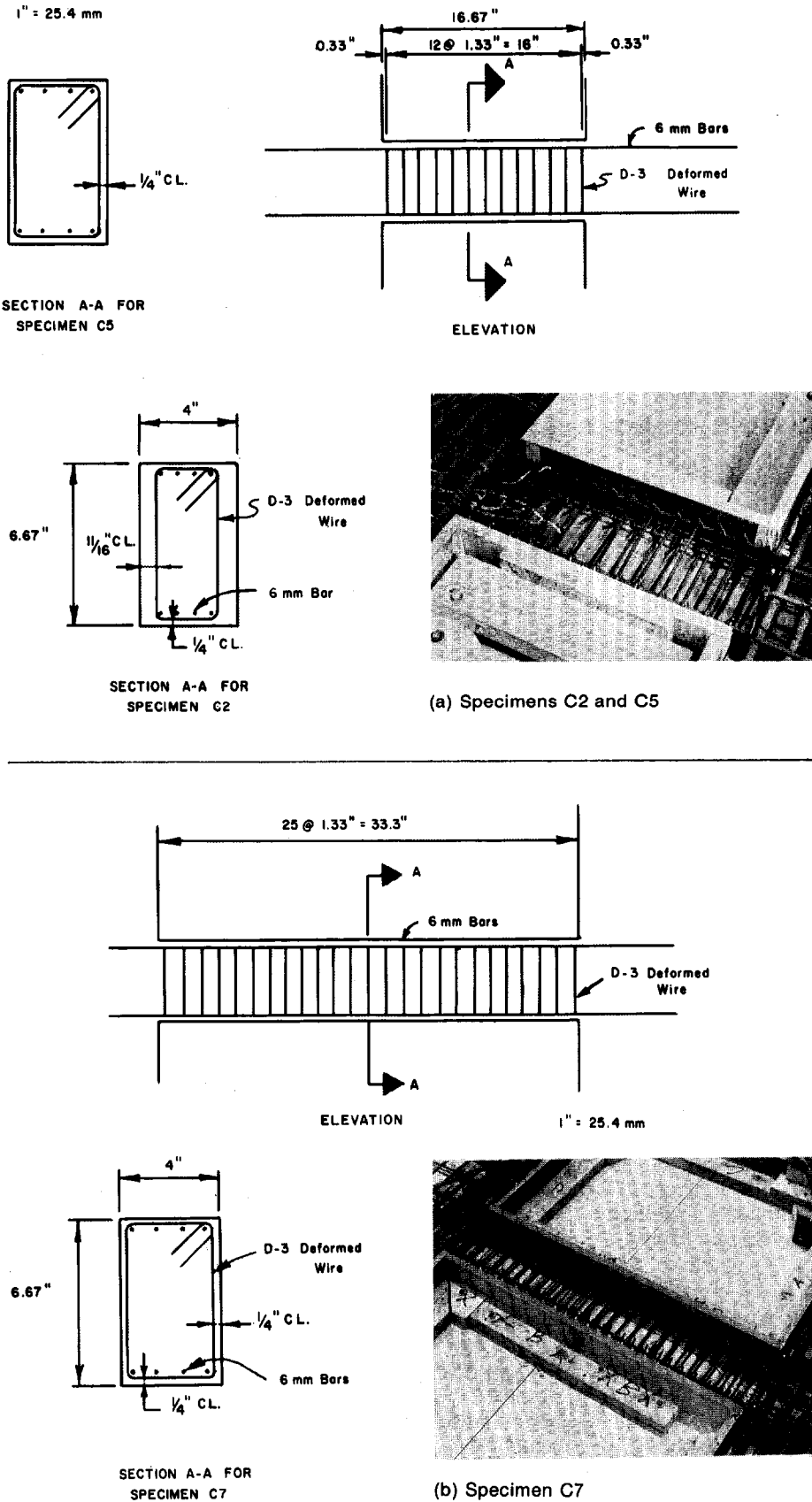
4. Wight, J. K., and Sozen, M. A., "Strength Decay of RC Columns Under Shear Reversals," *Journal of the Structural Division*, American Society of Civil Engineers, Vol. 101, No. ST5, May 1975, pages 1053-1065.
5. ACI Committee 318, Building Code Requirements for Reinforced Concrete, ACI Standard 318-71, American Concrete Institute, Detroit, 1971, 78 pages.
6. Barney, G. B.; Shiu, K. N.; Rabbat, B. G.; Fiorato, A. E.; Russell, H. G., and Corley, W. G., "Earthquake Resistant Structural Walls—Tests of Coupling Beams," Portland Cement Association, January 1978, National Technical Information Service, U.S. Department of Commerce, Springfield, Va. (NTIS Accession No. PB-293 542/7WB).
7. Bachmann, H., "Influence of Shear and Bond on Rotational Capacity of Reinforced Concrete Beams," International Association for Bridge and Structural Engineering, Vol. 30, Part II, Zurich, 1970, pages 11-28.
8. Standard Specification for Deformed and Plain Billet-Steel Bars for Concrete Reinforcement, A615-76a, American Society for Testing and Materials, Philadelphia.
9. Hognestad, E.; Hanson, N. W.; Kriz, L. B.; and Kurvits, O., *Facilities and Test Methods of PCA Structural Laboratory*, Development Department Bulletin DX33, Portland Cement Association, 1959.

### APPENDIX: EXPERIMENTAL PROGRAM

Details of the experimental program including specimen geometry, reinforcement details, material properties, fabrication, and testing are given in this Appendix.

#### Test Specimens

Eight specimens representing approximately one-third scale models of coupling beams were tested. Each specimen consisted of two coupling beams framing into rigid abutment walls at each end as shown in Fig. 3. The end conditions imposed by the abutments simulated those in a structural wall system.



Coupling beams had rectangular cross sections 4 in. (102 mm) wide and 6.67 in. (169 mm) deep. The beams were either 16.67 in. (423 mm) or 33.33 in. (846 mm) long, corresponding to span-to-depth ratios of 2.5 and 5.0, respectively. The L-shaped abutments were 4 in. (102 mm) thick.

**Details of Reinforcement**

Steel reinforcement details are presented in Figs. A-1 through A-3.

**Specimens C2, C5, and C7.** Primary reinforcement in Specimens C2, C5, and C7 consisted of four straight longitudinal 6-mm-diameter (1/4-in.) bars, top and bottom. Reinforcement details are shown in Fig. A-1. Specimens C2 and C5 had a shear span-to-effective-depth ratio of 1.4. The shear span-to-effective-depth ratio for Specimen C7 was 2.8. Specimens C5 and C7 had a confined concrete core size about 33% larger than that of Specimen C2. To obtain the increase in core size without bending the bars, it was necessary to place the straight flexural bars in the coupling beams outside the reinforcement in the abutment walls. Therefore, these bars were not anchored in confined concrete. This anchorage detail, although satisfactory for the test, is not recommended for field practice.

**Specimen C1.** Diagonal reinforcement was provided for Specimen C1 as shown in Fig. A-2. Two 6-mm-diameter (1/4-in.) bars top and bottom were bent at 45° starting at the face of the wall at each end of the beam.

**Specimens C3 and C4.** Diagonals were provided in the hinging regions of Specimens C3 and C4 as shown in Fig. A-2. Four 6-mm-diameter (1/4-in.) bars were bent at 45° top and bottom. Specimens C3 and C4 were similar except for the size of the confined concrete core. Specimen C4 had a core area 33% greater than Specimen C3, as shown in Fig. A-2. The larger core size required that the top and bottom reinforcing bars in the coupling beams be placed outside the steel in the rigid abutments. This anchorage detail is not recommended for field practice.

**Specimens C6 and C8.** Primary reinforcement for Specimens C6 and C8 consisted of full-length diagonals as shown in Fig. A-3. Diagonals were two

Fig. A-1. Details for beams with conventional reinforcement.

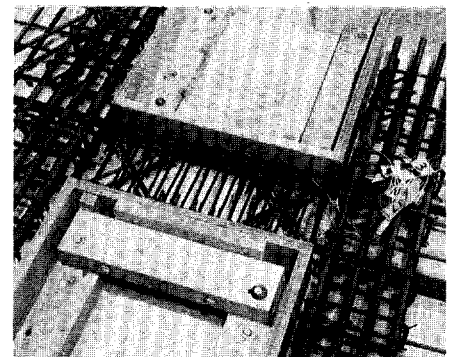
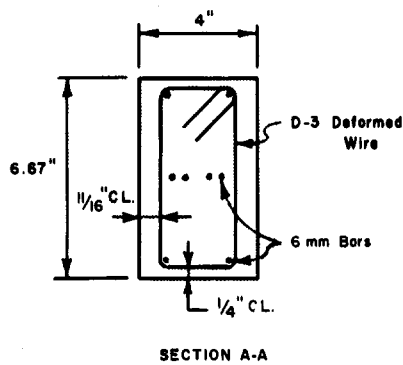
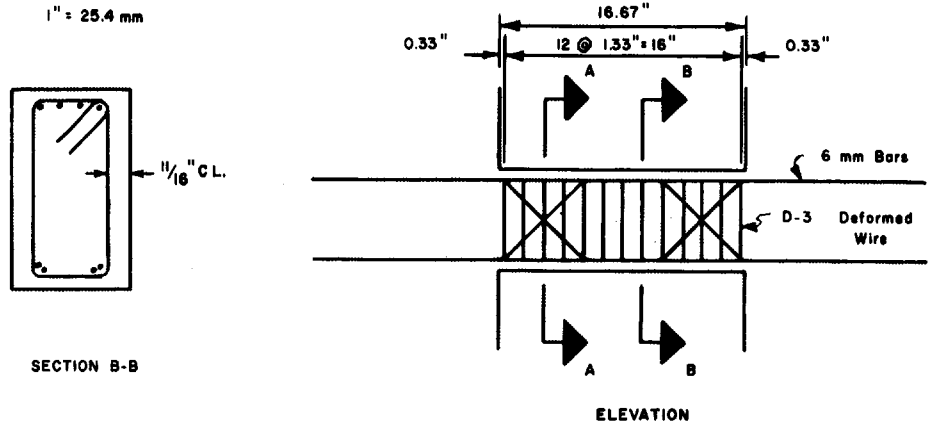
No. 3 bars in one direction and one No. 4 bar in the other. Symmetry was maintained by passing the No. 4 bar between the No. 3 bars at midspan. Two 6-mm-diameter (1/4-in.) longitudinal bars were provided for tying hoops in place. These bars were not anchored in the abutment walls.

**Materials**

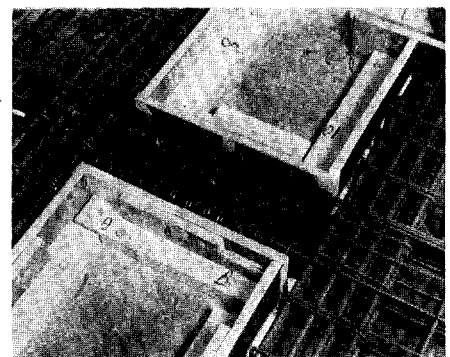
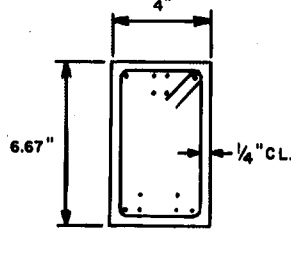
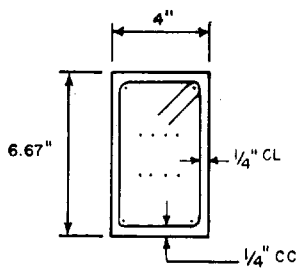
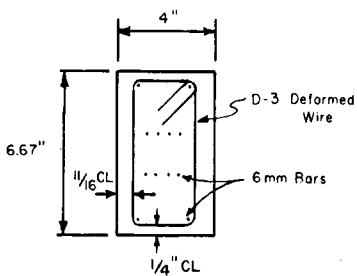
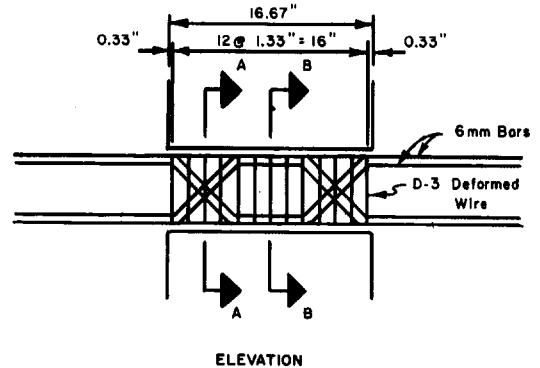
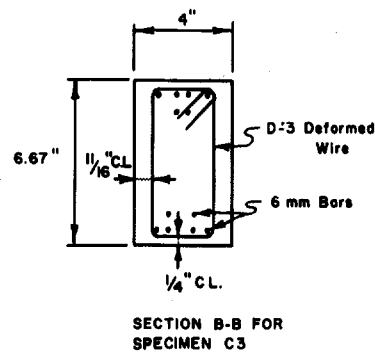
Concrete and reinforcing steel properties for the test specimens are summarized in Table A-1.

Concrete was designed for a compressive strength of 3000 psi (20.7 MPa). The mix consisted of Type I cement, sand, and aggregate with a maximum size of 3/8 in. (9.5 mm). Material properties were determined from tests on 6x12-in. (153x305-mm) cylinders. Concrete properties are contained in Table A-1 and a representative stress-versus-strain curve is shown in Fig. A-4.

For the reinforcement, No. 3 and No. 4 bars conformed to ASTM Designation A615 Grade 60.<sup>(8)</sup> Deformed 6-mm (1/4-in.) hot-rolled bars with properties similar to those of Grade 60 bars were also used as primary reinforcement. Deformed wire, size D-3, was used for transverse hoops. This wire was heat-treated to obtain stress-strain characteristics similar to those of Grade 60 bars. Physical properties of the reinforcement used in the test specimens are given in Table A-1. Representative stress-versus-strain relationships are shown in Fig. A-5.



(a) Specimen C1



(b) Specimens C3 and C4

Fig. A-2. Details for beams with bent diagonal reinforcement.

**Fabrication**

Specimens were cast in a horizontal position using the forming system shown in Fig. A-6. Reinforcing cages for the abutments and coupling beams were constructed separately and then placed together in the form. Before casting, lifting eyes and inserts for attaching external instrumentation were placed in position.

Each specimen was cast in four batches. Concrete for both coupling beams in each specimen was taken from the same batch. After casting, the specimens were covered with a sheet of polyethylene plastic and allowed to cure for 4 days. Control cylinders were cured similarly. Specimens were then stripped and moved to the test location. Testing usually began on the fourteenth day after casting.

**Supporting and Loading Systems**

Specimens were placed parallel to the laboratory floor<sup>(9)</sup> and supported on thrust bearings as illustrated in Fig. A-7. Blocks to resist applied forces were post-tensioned to the laboratory floor on each side of the specimen. One end of the specimen was fixed. Hydraulic rams were used to apply load at the opposite end. The line of action of the applied forces passed through the midspan of the coupling beams. This minimized the possibility of axial forces occurring in the beams.

Magnitude of the applied forces was controlled by a hydraulic pump. A four-way valve was used in the hydraulic line for directing pressure to one of two rams to either push or pull on the specimen. Lateral movement at the live end of the specimens was prevented by roller guides bearing against blocks stressed to the laboratory floor.

**Instrumentation**

Test specimens were instrumented to measure applied and resisted loads, deflections, and steel strains. Readings from each sensing device were recorded by a digital data acquisition system interfaced with a desk-top microcomputer. Data were stored in cassettes.

Loads were recorded by local cells<sup>(9)</sup> located at both the fixed and live ends of the specimens. This arrangement provided a means for determining losses

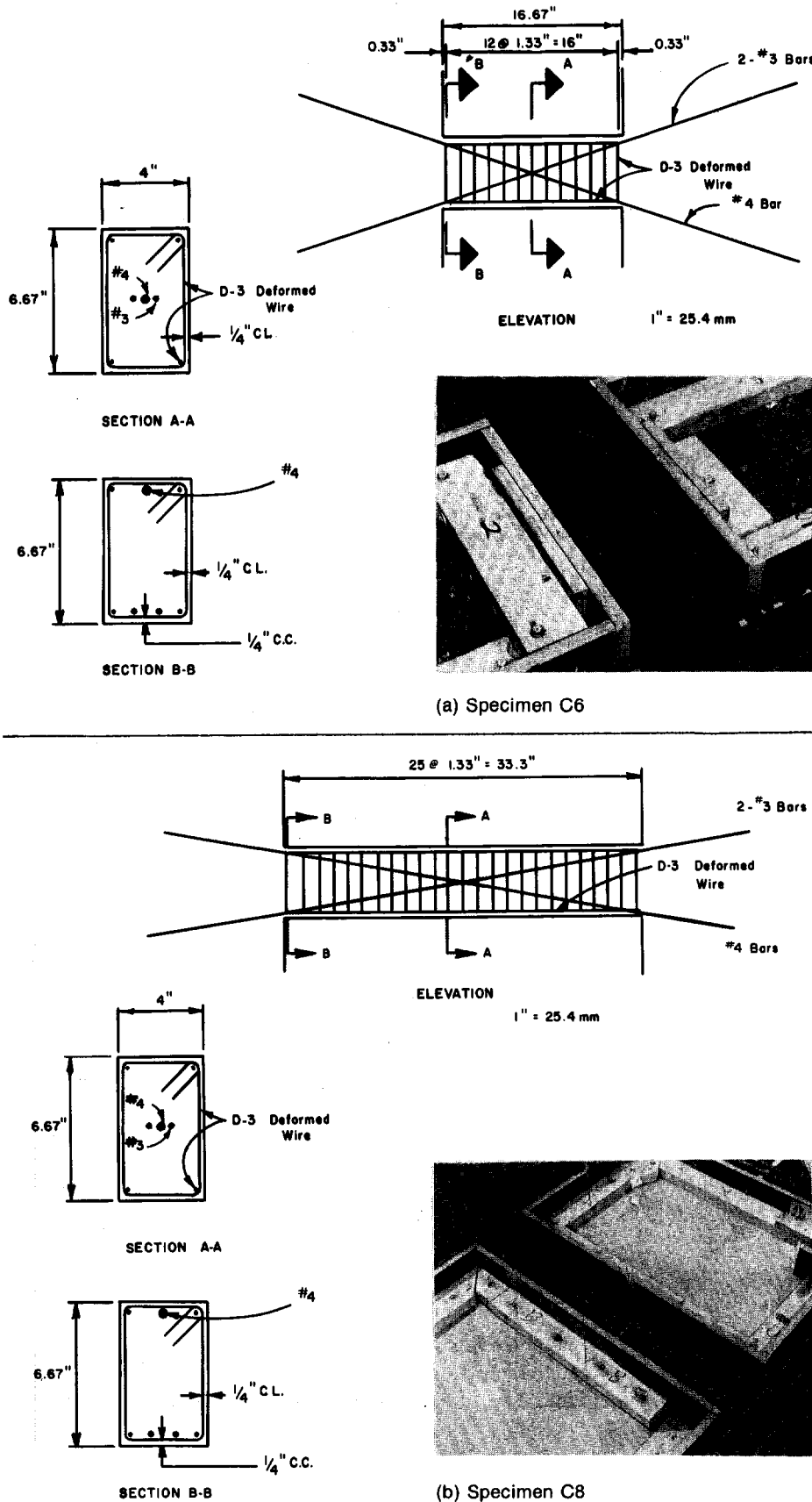


Fig. A-3. Details for beams with full-length diagonal reinforcement.

**TABLE A-1. Material Properties**

Specimen No.	D-3* deformed wire (ksi)			6-mm** bar (ksi)			No. 3 bar (ksi)			No. 4 bar (ksi)			Concrete	
	$f_y$	$f_{su}$	$E_s$	$f_y$	$f_{su}$	$E_s$	$f_y$	$f_{su}$	$E_s$	$f'_c$	$f_{su}$	$E_s$	$f'_c$ (psi)	$E_c$ (ksi)
C1	70.0	76.3	32,400	69.2	98.0	31,400	—	—	—	—	—	—	2940	3180
C2	69.3	75.0	30,000	74.9	99.8	30,000	—	—	—	—	—	—	3050	2910
C3	69.3	75.1	29,400	73.6	98.8	30,600	—	—	—	—	—	—	2970	3040
C4	70.8	75.0	31,300	66.0	89.7	30,000	—	—	—	—	—	—	3490	3170
C5	71.1	75.1	31,100	66.3	88.8	30,000	—	—	—	—	—	—	3140	2730
C6	71.4	75.1	31,000	—	—	—	70.7	104.7	30,200	59.2	103.2	31,000	2620	2780
C7	62.1	72.5	26,700	66.5	87.8	30,800	—	—	—	—	—	—	3710	3050
C8	71.0	81.7	28,300	—	—	—	82.5	125.1	28,600	62.8	102.5	28,500	3470	3100

$f_y$  = yield strength of steel  
 $f_{su}$  = tensile strength of steel  
 $E_s$  = modulus of elasticity of steel

$f'_c$  = compressive strength of concrete  
 $E_c$  = modulus of elasticity of concrete  
 1000 psi = 1 ksi = 6.895 MPa

\*Area = 0.03 sq in. (19 mm<sup>2</sup>)  
 \*\*Area = 0.05 sq in. (32 mm<sup>2</sup>)

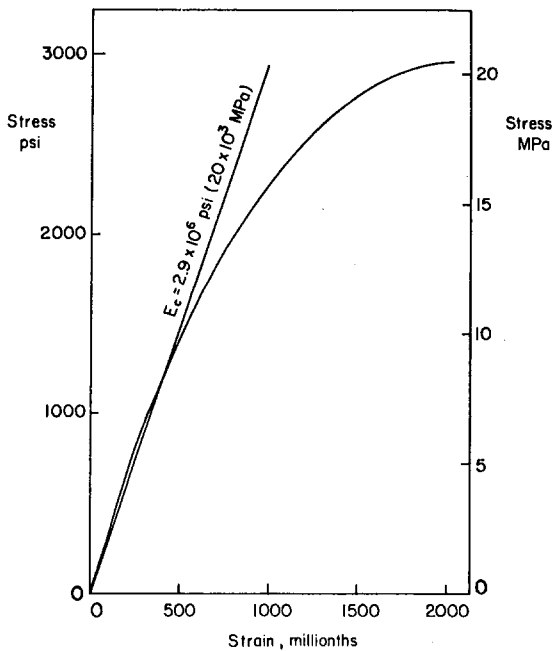


**Fig. A-4. Representative stress-versus-strain relationship for concrete.**

caused by friction in the thrust-bearing supports. Loss was generally less than 2% of the applied loads.

Lateral displacements in most specimens were recorded at three locations. The sensitivity of the gages was 0.001 in. (0.03 mm). One gage was attached to brackets on the inside face of each rigid abutment midway between the coupling beams, as shown in Fig. A-8. Two additional gages were installed at the end of

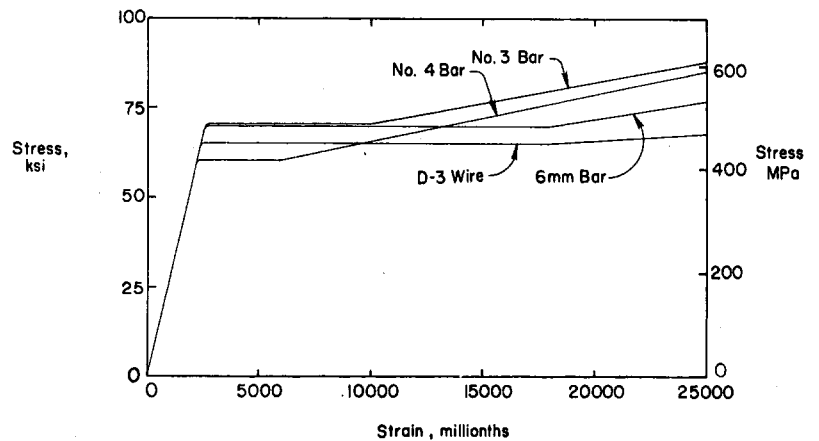


**Fig. A-5. Representative stress-versus-strain relationships for reinforcement.**

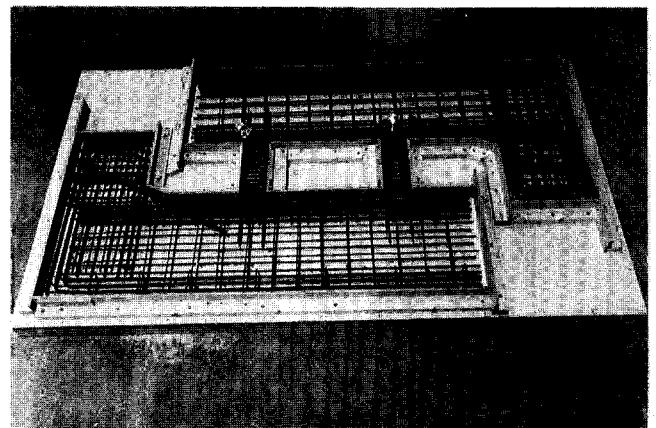


**Fig. A-6. Specimen prior to casting.**

each coupling beam. All three gages measured the relative lateral displacement of the ends of the coupling beams. Gages were also installed to measure axial deformations at each coupling beam location.

A continuous record of load versus deflection was also recorded by an XY plotter. Load was measured by calibrated pressure cells. Deflections were taken as the relative lateral movement between the abutment walls.

**Test Procedure**

Prior to yield, loading was controlled by the magnitude of applied forces. After yielding, loading was controlled by the imposed deflection on specimens.

Three complete loading cycles were applied for each predetermined level of force or displacement. The combined three cycles are termed a load increment. Each cycle started and ended with zero force applied.

The first cycle of each increment was applied in steps termed load stages. Data were recorded at each load stage. On the second and third cycles, data were recorded only at peak loads or displacements.

Testing was terminated either when a significant loss of capacity occurred or when specimens experienced bar fracture.

After each load stage, specimens were inspected visually for cracking and evidence of distress. Cracks were marked with a felt-tip pen. Photographs were taken at the end of each load stage to provide a record of crack development.

**Test Results**

Test results are given in the body of this report and have also been published in detail elsewhere.<sup>(6)</sup>

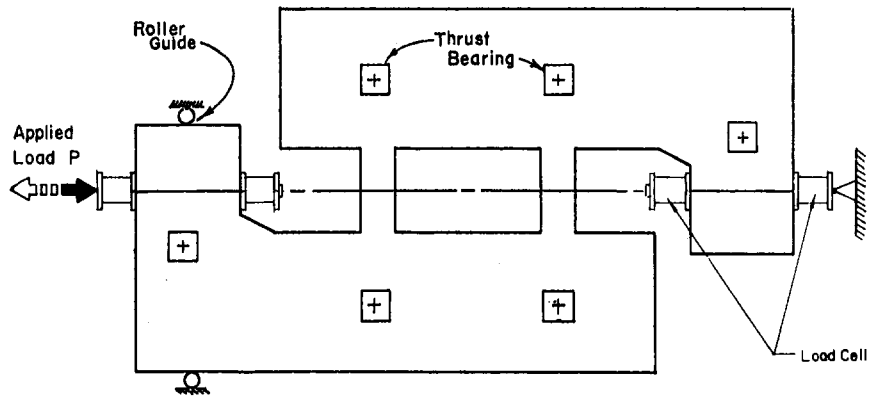


Fig. A-7. Test setup.

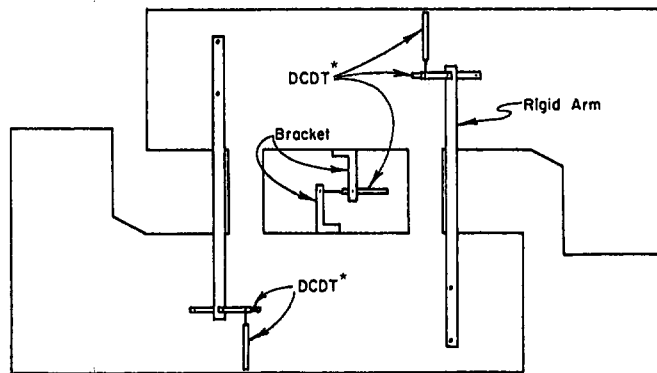


Fig. A-8. External instrumentation.

\*Direct-current differential transformer

This publication is based on the facts, tests, and authorities stated herein. It is intended for the use of professional personnel competent to evaluate the significance and limitations of the reported findings and who will accept responsibility for the application of the material it contains. The Portland Cement Association disclaims any and all responsibility for application of the stated principles or for the accuracy of any of the sources other than work performed or information developed by the Association.

**KEYWORDS:** beams, buildings, concrete (reinforced), deformation, earthquake resistant structures (forces), loads (forces), reinforced concrete, reinforcement (structures), shear strength, shear stress, structural design, tests.

**ABSTRACT:** Describes tests of eight model reinforced concrete coupling beam specimens subjected to reversing loads to determine load versus deflection; strength; energy dissipation; and ductility. The effects of shear span-to-effective-depth ratio, reinforcement details, and size of confined concrete core on hysteretic response were determined. Full-length diagonal reinforcement improved performance of short beams. Larger concrete core increased load-retention capacity.

**REFERENCE:** Barney, G. B., and others, *Behavior of Coupling Beams Under Load Reversals* (RD068.01B), Portland Cement Association, 1980.

PORTLAND CEMENT  ASSOCIATION

An organization of cement manufacturers to improve and extend the uses of portland cement and concrete through scientific research, engineering field work, and market development.

5420 Old Orchard Road, Skokie, Illinois 60077